The European Zoological Journal

ISSN: (Print) (Online) Journal homepage: https://www.tandfonline.com/loi/tizo21

Chelarctus and *Crenarctus* (Crustacea: Scyllaridae) from Coral Sea waters, with molecular identification of their larvae

R. Genis-Armero, M. Błażewicz, P. F. Clark & F. Palero

To cite this article: R. Genis-Armero, M. Błażewicz, P. F. Clark & F. Palero (2022) *Chelarctus* and *Crenarctus* (Crustacea: Scyllaridae) from Coral Sea waters, with molecular identification of their larvae, The European Zoological Journal, 89:1, 446-466, DOI: 10.1080/24750263.2022.2036256

To link to this article: https://doi.org/10.1080/24750263.2022.2036256

Published online: 22 Mar 2022.

The European Zoological Journal, 2022, 446–466
Vol. 89, No. 1, https://doi.org/10.1080/24750263.2022.2036256

Chelarctus and *Crenarctus* (Crustacea: Scyllaridae) from Coral Sea waters, with molecular identification of their larvae

R. GENIS-ARMERO [1,2], M. BŁAŻEWICZ [2], P. F. CLARK [3], & F. PALERO [1,3,*]

[1]*Cavanilles Institute of Biodiversity and Evolutionary Biology, University of Valencia, Paterna, Spain,* [2]*Department of Invertebrate Zoology and Hydrobiology, Faculty of Biology and Environmental Protection, University of Lodz, ul. Banacha 12/16, 90-237, Łódź, Poland, and* [3]*Department of Life Sciences, The Natural History Museum, Cromwell Road, SW7 5BD, London, England*

(Received 12 Jul 2021; accepted 25 Jan 2022)

Abstract
Chelarctus Holthuis, 2002 is widely distributed throughout the Indo-West Pacific, but its biogeographic patterns are unknown because Southern Hemisphere areas, such as the Coral Sea, remained poorly explored. Recent cruises organized by the Muséum national d'Histoire naturelle of Paris and the Australian Institute of Marine Science allowed the molecular identification of *Crenarctus crenatus* (Whitelegge, 1900), *Chelarctus aureus* (Holthuis, 1963) and *Chelarctus crosnieri* Holthuis, 2002 phyllosomae. The Coral Sea *C. crenatus* larvae are identical to stages IX and X of *Scyllarus* sp. Z, described in detail by Webber and Booth (2001). Descriptions of phyllosoma stages VI, IX and X of *Ch. aureus* and stages IX and X of *Ch. crosnieri* are also presented here. Morphological differences between *Crenarctus* and *Chelarctus* larvae are established for the first time and previous misidentifications in the literature are re-assessed.

Keywords: *Decapoda, DNA barcoding, slipper lobster, Indo-West Pacific*

Introduction

Although biogeographic barriers are well defined for terrestrial species (Lohman et al. 2011) comparatively fewer studies have addressed Indo-West Pacific (IWP) marine boundaries, which require clarification. Plate tectonics and sea level changes have been claimed to account for phylogeography patterns in the area (Hou & Li 2018), but historical factors and spatial boundaries may not equally affect shallow water (Lourie & Vincent 2004; Palero et al. 2016a) and deep-water taxa (Tsoi et al. 2011). Previous studies usually focused on limited areas or bathymetric ranges, however, further taxa should be analysed to better understand IWP marine biogeography (Lourie et al. 2005; Barber et al. 2006; Kochzius & Nuryanto 2008). The Indo-West Pacific biodiversity hotspot (Hall 2002) hosts representatives from almost every slipper lobster genus, a group of decapod crustaceans expanding from shallow waters to the continental slope (Holthuis 1991). Slipper lobsters (Scyllaridae Latreille, 1825) are a well-established monophyletic family characterized by their flattened distal antennal article (Holthuis 1985; Haug et al. 2016), but relationships between genera and species still remain unresolved (Yang et al. 2012; Bracken-Grissom et al. 2014). The existence of slipper lobster species yet to be described is ensured by their cryptic coloration and small size, together with the fact that they occupy habitats such as coral reefs and underwater caves.

Chelarctus Holthuis, 2002 includes a total of four species and it is widely distributed throughout IWP waters, occupying hard and muddy bottoms at depths down to >300 m. The northernmost species, *Ch. virgosus* Yang & Chan, 2012, inhabits shallow areas (<50 m) from Japan and northern Taiwan. *Chelarctus cultrifer* (Ortmann, 1897) and *Ch. aureus*

*Correspondence: F. Palero Cavanilles Institute of Biodiversity and Evolutionary Biology, University of Valencia, Paterna, Spain; Department of Life Sciences, The Natural History Museum, Cromwell Road, London SW7 5BD, England. Email: Ferran.Palero@uv.es

(Holthuis, 1963) are mostly distributed along continental slopes (50–250 m) of the Coral Triangle and the Tropical Southwestern Pacific (TSWP) provinces, respectively (Holthuis 2002). Molecular data recently revealed two genetic clusters within *Ch. cultrifer*, but morphological analyses did not establish specific status to these groups (Yang & Chan 2012). Furthermore, *Ch. crosnieri* Holthuis, 2002 occupies deeper waters (>250 m) from the southern hemisphere and it is only known from a few specimens (Figure 1). Another genus found in shallow waters of the IWP is *Crenarctus* Holthuis, 2002, which currently includes *Cr. bicuspidatus* (Ortmann, 1897), distributed from Japan to New Caledonia, and *Cr. crenatus* (Whitelegge, 1900) from southeast Australia (Holthuis 2002). Recent molecular results and adult morphology suggest that the eastern Pacific species *Acantharctus delfini* (Bouvier, 1909) should be assigned to *Crenarctus* (Genis-Armero et al. 2020). Campaigns carried out by the Muséum national d'Histoire naturelle, Paris (MNHN) in the Vanuatu archipelago (SANTO 2006), Papua New Guinea (BIOPAPUA 2010 and PAPUA NIUGINI 2012–2013) and New Caledonia (KANADEEP 2017) have now provided new regional data (Chan 2012; De Forges & Corbari 2012; Pante et al. 2012; Zaharias et al. 2020). In parallel, the Australian Institute of Marine Science (AIMS) launched several cruises to collect marine plankton from the Coral Sea area. These cruises have successfully collected hundreds of scyllarid phyllosoma (Palero et al. 2014, 2016b), most of which await study.

The phyllosoma is the larval form of slipper and spiny lobsters, particularly adapted to planktonic life and long-distance dispersal (Palero & Abello 2007). Difficulties distinguishing these larvae make generic identifications based on morphological highly unreliable. For example, Higa and Shokita (2004) have assigned putative *Cr. bicuspidatus* (De Man 1905) phyllosoma from previous works to *Ch. cultrifer*, but Wakabayashi et al. (2020) suggest that *Ch. cultrifer* phyllosoma described by Higa and Shokita (2004) and Inoue and Sekiguchi (2006) belong in fact to *Ch. virgosus*. Ueda et al. (2021) recently studied *Chelarctus* larvae from northern and central Pacific waters but, apparently due to the poor status of their specimens, illustrations and descriptions were deficient and their morphological results remain inconclusive.

The purpose of the present study is to identify Coral Sea phyllosoma samples collected during cruises 5441 and 5160 (AIMS) and the KANADEEP 2017 cruise (MNHN). Two mitochondrial (COI and 16S rDNA) and one nuclear (18S) marker are used to distinguish between larval stages of *Chelarctus* and *Crenarctus* species. Once identified, developmental stages of *Chelarctus* species are described, highlighting key morphological characters to discriminate taxa and revising larval identities from previous reports.

Material and methods

Phyllosomae used for molecular analysis and descriptions were obtained by AIMS during Cruise

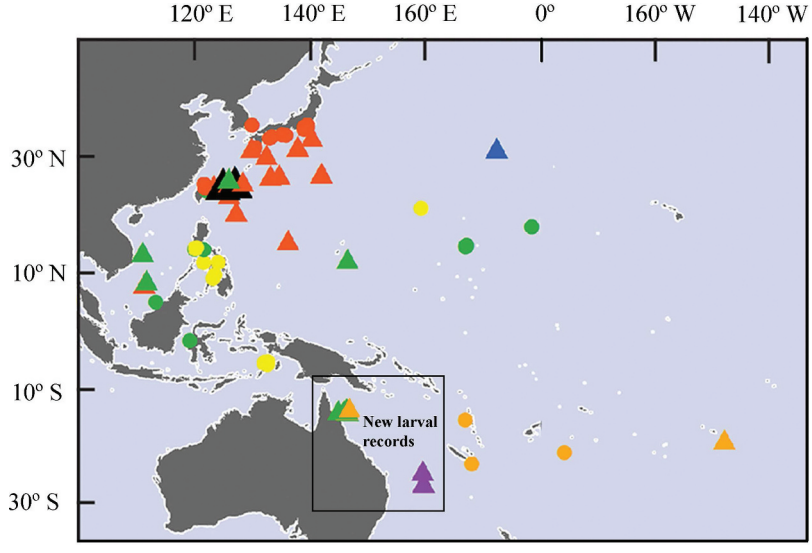

Figure 1. Localities where *Chelarctus* and *Crenarctus* larvae (triangles) and adults (circles) have been reported from the Indo-West Pacific. Green: *Chelarctus aureus*; orange: *Ch. crosnieri*; yellow: *Ch. cultrifer*; red: *Ch. virgosus*; black: *Chelarctus* sp.; purple: *Crenarctus crenatus* and blue: *Crenarctus* sp.

Table I. Sampling locations from Indo-West Pacific waters where *Chelarctus* and *Crenarctus* larvae have been reported. Sampling information includes cruise, station, date, coordinates and original reference.

Cruise	Station	Date	Longitude	Latitude	Reference
C5160	15	27/5/12	13°46' S	146°27'E	Present study
	26	26/5/12	13°44' S	146°25' E	
	50	28/5/12	14°06' S	146°42' E	
	413	6/6/11	-	-	
C5441	68	20/7/12	13°47' S	146°33' E	
	142	21/7/12	13°48' S	146°36' E	
	159	21/7/12	13°47' S	146°35' E	
	175	22/7/12	13°47' S	146°32' E	
	181	22/7/12	13°47' S	146°34' E	
	205	22/7/12	13°50' S	146°38' E	
C4922	-	10–19/5/2010	14°00' S	146°40' E	
KANADEEP	CP4937	4/9/17	25°26' S	159°47' E	
	CP4947	5/9/17	24°06' S	159°37' E	
RV SHUNYO-MARU	2a	23/6/09	25°33' N	127°02' E	Ueda et al. 2021
	7	8/6/09	25°30' N	126°05' E	
	20a	19/6/09	25°16' N	124°68' E	
	22	9/6/09	23°19' N	126°09' E	
	23	10/6/09	26°09' N	126°01' E	
RV KOYO-MARU	-	30/1/15	27°07' N	142°05' E	
	-	31/1/15	27°02' N	142°05' E	
RV HAKUHO-MARU	226	11/9/16	19°00' S	147°30' W	
-	-	31/5/84	25°39' N	128°31' E	Inoue & Sekiguchi 2006
	-	16/6/84	26°43' N	133°19' E	
	-	5/8/84	30°15' N	132°34' E	
	-	5/11/86	31°29' N	129°59' E	
	-	16/6/84	26°43' N	133°19' E	
NAGASAKI MARU	Site N-1	23/11/89	24°58' N	123°29' E	Higa & Shokita 2004
	Site N-1	23/11/98	24°58' N	123°29' E	
	Site N-1	23/11/98	24°58' N	123°29' E	
KEITEN MARU	-	11/11/98	26°51' N	134°47' E	
	-	15/6/98	15°59' N	136°18' E	
-	-	1969–92	36°52' S	178°27' E	Webber & Booth 2001
83-R-10	-	25/9-8/1/83	32°59' N	135°45' E	Sekiguchi 1986
	-		34°27' N	137°56' E	
	-	13–21/9/84	32°20' N	135°45' E	
	-		34°45' N	138°45' E	

5160, from 24th May to 10th June 2011, and Cruise 5441, between 16th and 26th July 2012. Both cruises were carried out in the vicinity of Osprey Reef, a submerged atoll which rises from a depth of about 2,000 m in the Coral Sea. The reef is about 200 km off the eastern coast of northeast Queensland, with the nearest reefs approximately 60 km away. Specimens were stored directly in absolute ethanol at low temperature (−20°C), and later deposited in the Natural History Museum, London (NHM). In addition, during the KANADEEP 2007 cruise organized by the MNHN, larval specimens were collected from temperate waters south of the Coral Sea. These specimens were included in our molecular and morphological analyses, and they are kept in the MNHN collections (MNHN-IU-2017-2420 and MNHN-IU-2017-10,460). Station number, latitude, longitude and sampling date, together with data from AIMS and KANADEEP, and previous campaigns available in the literature, are detailed in Table I and Supplementary Table.

Molecular analyses

Total genomic DNA extraction was performed using the Chelex-resin method (Palero et al. 2010) from a single pereiopod of each larva. One nuclear (18S) and two mitochondrial (COI and 16S) genes were used to identify the larvae and reconstruct phylogenetic relationships within *Chelarctus*, using standard universal primers previously tested in Achelata (Palero et al. 2008, 2009; Bracken-Grissom et al. 2014). After observing significant intraspecific variation for COI and considering

Ueda et al. (2021) reported difficulties using standard universal primers for DNA barcoding (Folmer et al. 1994), COI was also amplified using a new pair of primers proposed by Krehenwinkel et al. (2018), ArF1: 5' – GCNCCWGAYATRGCNTTYCCNCG – 3' (Gibson et al. 2014) and Fol-degen-rev: 3' – TANACYTCNGGRTGNCCRAARAAYCA – 5' (Yu et al. 2012). Amplifications were carried out using ~30 ng of genomic DNA in a reaction containing 1 U of Taq polymerase (Amersham), 1 × buffer (Amersham), 0.2 mM of each primer and 0.12 mM dNTPs. The polymerase chain reaction (PCR) thermal profile was 94°C for 4 min for initial denaturation, followed by 30 cycles of 94°C for 30s, 50°C for 30s, 72°C for 30s and a final extension at 72°C for 4 min. Sequences were obtained using the Big-Dye Ready-Reaction kit ver. 3.1 (Applied Biosystems) on an ABI Prism 3770 automated sequencer at the NHM sequencing facilities. Chromatograms for each DNA sequence were checked with BioEdit v7.2.5 (Hall 1999) and sequence alignment was conducted using the program Muscle v3.6 (Edgar 2004) with default parameters. Model selection was performed according to the BIC criterion as implemented in MEGA X (Kumar et al. 2018). The construction method of maximum-likelihood (ML) phylogenetic tree was applied as implemented in PhyML v.3.0 (Guindon et al. 2010). K2P genetic distances were also estimated for COI and 16S genes dataset using MEGA X (Kumar et al. 2018), in order to allow for comparison with previous values in the bibliography.

Morphological description

Drawings of whole larvae and appendages were made with a *camera lucida* attached to a Leica M165C high-performance stereo microscope (Leica Microsystems, Germany). Antennules, mouth appendages (including paragnaths and mandibles), maxillipeds and pereiopods were individually dissected for an accurate description and because they might convey information of taxonomic value (pers. obs). An Intuous-S graphic tablet (Wacom) and Adobe Illustrator (https://adobe.com/products/illustrator) were used for digitalization of drawings following Coleman (2003, 2009). The sequence of larval descriptions was based on the malacostraca somite plan and described from anterior to posterior and proximal to distal (Clark et al. 1998). Boxshall (2004) has challenged the traditional description of the Malacostraca antennule developing from a uniramous appendage to a biramous structure with endopod and exopod. The terminology biramous is considered inappropriate for the antennule, and instead of exopod and endopod, the terms primary and accessory flagella should be used (see Boxshall et al. 2010 for review). Setae nomenclature follows Garm and Watling (2013). Stage division was made on the basis of morphological development and changes in total length (Genis-Armero et al. 2020). Body length (BL) was measured from anterior margin of cephalic shield between the eyes to posterior margin of telson; cephalic length (CL) from anterior to posterior margin of cephalic shield, cephalic width (CW) measured at widest part of cephalic shield, thorax length (TL) from anterior to posterior margin of thorax, thorax width (TW) measured at the widest part of thorax shield, pleon length (PL) from anterior to posterior margin of pleon, and pleon width (PW) measured as the distance between insertion points of fifth pereiopods (P5). Morphometric measurements were obtained using the software ImageJ (Schneider et al. 2012). Different morphological characters were used to define genera and species groups following previous studies (Maigret 1978; Phillips & McWilliam 1986; Webber & Booth 2001; Inoue & Sekiguchi 2006), cephalon posterior margin (CPM), cephalon shape (CS), articulation of fifth pereiopod (P5), thoracic dorsal spines (TDS), and CL/CW ratio. The new characters proposed here with taxonomic value for *Chelarctus* and *Crenarctus* were, the cephalon edge (CE), relative length of carpus and propodus of maxilliped 3 (Crp/Prd) and PL/PW and BL/CW ratios. The set of morphological characters are detailed in Table II.

Results

Molecular analyses

New sequences obtained from the phyllosoma larvae have been deposited in GenBank under accession numbers: MZ452434-MZ452440 (COI Folmer), OM534650-OM534652 (COI Krehenwinkel), MZ460954-MZ460961 (16S rDNA) and MZ452441-MZ452444 (18S rDNA). Given the concerns raised by COI sequences obtained using Folmer universal primers (see below), only COI sequences obtained with the recent Krehenwinkel primer pair were used in the phylogenetic analyses. Total length of the concatenated alignment was 1699 bp, with 32.8% (555 bp) corresponding to the COI gene (Krehenwinkel primer pair), 23.2% (395 bp) to the 16S rDNA, and 44% (748 bp) corresponding to the 18S rDNA. The model selected for the COI alignment was the T92 + G model (lnL = −2308.3968), with Gamma parameter

Table II. Phyllosoma larvae (final stage) assigned to *Chelarctus* and *Crenarctus* based on our morphological and molecular results. Original and true identification, cephalon posterior margin (CPM), cephalon edge (CE), carpus length/propodus length ratio of maxilliped 3 (Crp/Prd), P5 articulation, cephalon shape (CS), thoracic dorsal spines (TDS), body length (BL), morphometrics (CL/CW, BL/CW, PL/PW), region where the larvae were collected and original references.

Original identity	New identification	CPM	CE	Crp/Prd	P5	CS	TDS	BL (mm)	CL/CW	BL/CW	PL/PW	Region	References
Chelarctus aureus	*Ch. aureus* ⋆	convex	P2	1.1	3	kidney-shape	P2–P4	23–24.6	0.6	1	0.7	Coral Sea	Present study
Chelarctus aureus	*Ch. aureus* ⋆	convex	P2	-	4?	kidney-shape	-	23.0	0.7	1.1	0.8	Japan	Ueda et al. (2021)
Scyllarus sp. A	*Ch. aureus*	convex	P2	1.1	3	kidney-shape	P1–P4?	22.0	0.7	1.1	0.7	South China	Johnson (1971)
Chelarctus crosnieri	*Ch. crosnieri* ⋆	convex	P2	1.0	3	kidney-shape	P2–P4	18.4–19.5	0.7	1.1	0.8	Coral Sea	Present study
Chelarctus sp. 1	*Chelarctus* sp.⋆	convex	P2	2.0	4?	kidney-shape?	-	28.4	0.8	1.3	0.9	Japan	Ueda et al. (2021)
Chelarctus virgosus	*Ch. virgosus*	convex	P2	1.0	3	pentagonal	P1–P4	22.0	0.8	1.3	1.1	Taiwan	Present study
Chelarctus virgosus	*Ch. virgosus* ⋆	concave?	P2	1.0	4?	pentagonal	-	21.4	0.8	1.3	1.0	Japan	Ueda et al. (2021)
Chelarctus cultrifer	*Ch. virgosus*	convex	P2	-	4?	pentagonal	P1–P4	20.7	0.9	1.4	1.1	Japan	Inoue & Sekiguchi (2006)
Chelarctus cultrifer	*Ch. virgosus*	convex	P1?	1.1	4?	pentagonal	P1–P4	20.7	0.9	1.4	1.1	Taiwan	Higa & Shokita (2004)
Scyllarus bicuspidatus	*Ch. virgosus*	-	P2	1.0	3	pentagonal	P1–P4	25.0	0.8	1.3	1.0	Mariana	Sekiguchi (1990)
Scyllarus sp.	*Ch. virgosus*	convex	P2	0.9	3	pentagonal	P1–P4	21.0	0.8	1.3	1.2	Japan	Johnson (1979)
Scyllarus sp. A	*Ch. cultrifer* ?	convex	P2	-	3	pentagonal	P1–P4	21.0	0.8	1.3	1.0	South China	Johnson (1971)
Scyllarus delfini	*Cr. delfini*	straight	P1	0.5	4	rectangular	P1–P4	25.0	0.8	1.4	1.2	Juan Fernández Is.	Baez (1973)
Scyllarus sp. Z	*Cr. crenatus*	straight	P1	0.7	4	rectangular	P1–P4	18.6–30.5	0.8	1.3	1.2	New Zealand	Webber & Booth (2001)
Crenarctus crenatus	*Cr. crenatus* ⋆	straight	P1	0.7	4	rectangular	P1–P4	21.6	0.8	1.5	1.1	New Caledonia	Present study

(⋆) DNA barcoded

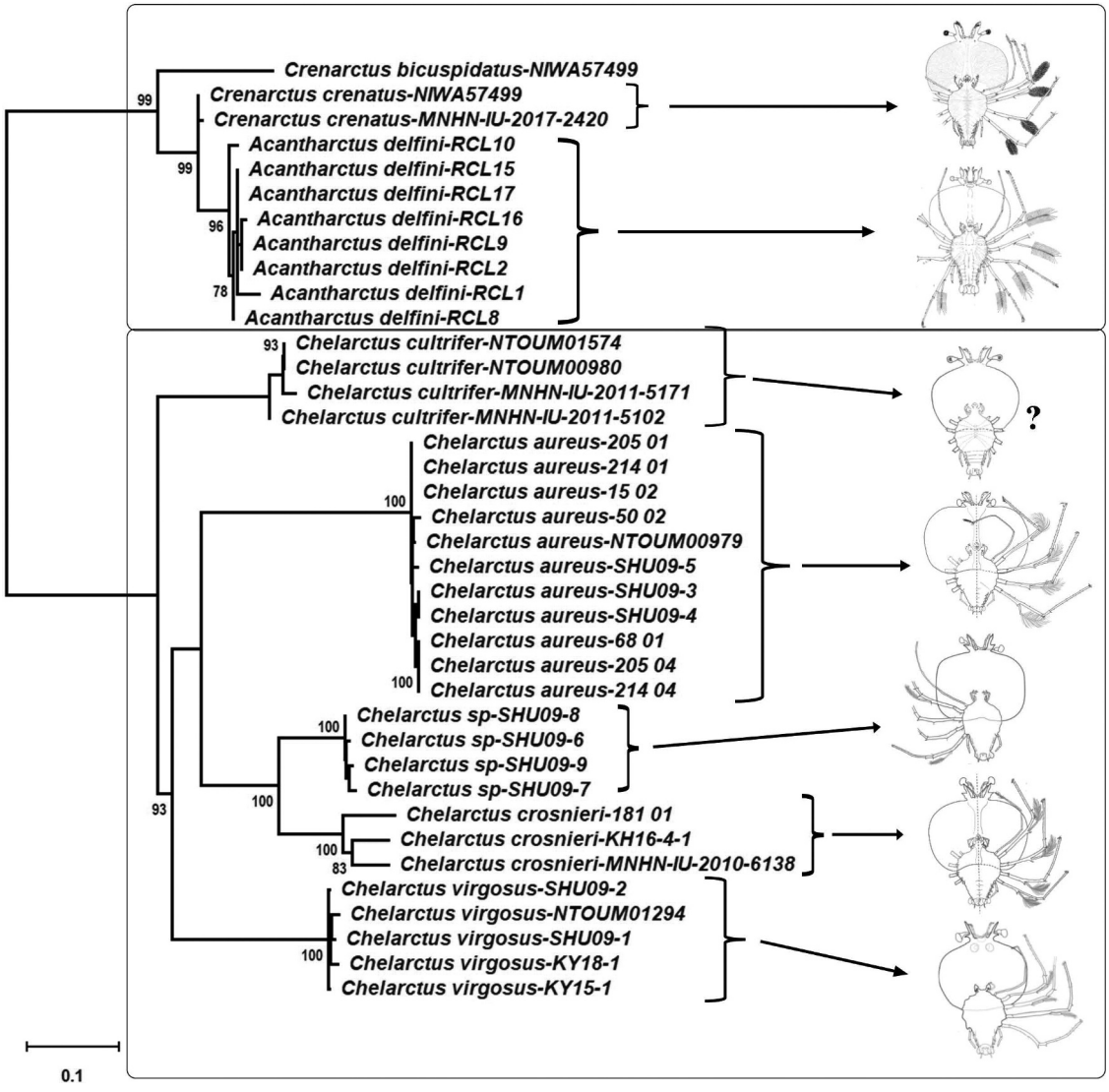

Figure 2. Maximum likelihood phylogenetic tree obtained from the concatenated alignment using 18S, 16S and COI genes of *Chelarctus* and *Crenarctus* specimens. Samples are detailed in the supplementary table except for the RCL larvae (see Palma et al. 2011). Larval images adapted from Johnson (1971), Baez (1973), Webber and Booth (2001) and Ueda et al. (2021). Only significant bootstrap values (>70) are shown.

(G = 0.1940), for 16S was HKY+G (lnL = −1198. 6509), with Gamma parameter (G = 0.1547) and JC model for 18S. Bootstrap results on the Maximum Likelihood tree strongly supported the species-level assignment of Coral Sea and New Caledonian larvae to *Ch. aureus*, *Ch. crosnieri*, and *Cr. crenatus* (Figure 2). In total, 11 phyllosomae have been identified using DNA barcoding as belonging to *Ch. crosnieri* (N = 2), *Ch. aureus* (N = 8) and *Cr. crenatus* (N = 1). For all *Chelarctus* larvae 18S genetic sequences were identical, 16S allowed to discriminate species but was identical between adults and larvae of both *Ch. aureus* and *Ch. crosnieri*, and only COI sequences showed intraspecific variation. Interestingly, COI genetic distances (K2P) between adult *Ch. aureus* from Taiwan and larvae from Coral Sea waters were much higher when using Folmer primers (0.165 ± 0.020) than the distance observed using the recent Krehenwinkel primer pair (0.020 ± 0.006), but this was not the case for *Ch. crosnieri* (0.090 ± 0.013 in both cases).

Morphological analyses

A list of the larvae used for molecular and morphological analysis, as well as previous larval records for *Chelarctus*, are shown in the Supplementary Table.

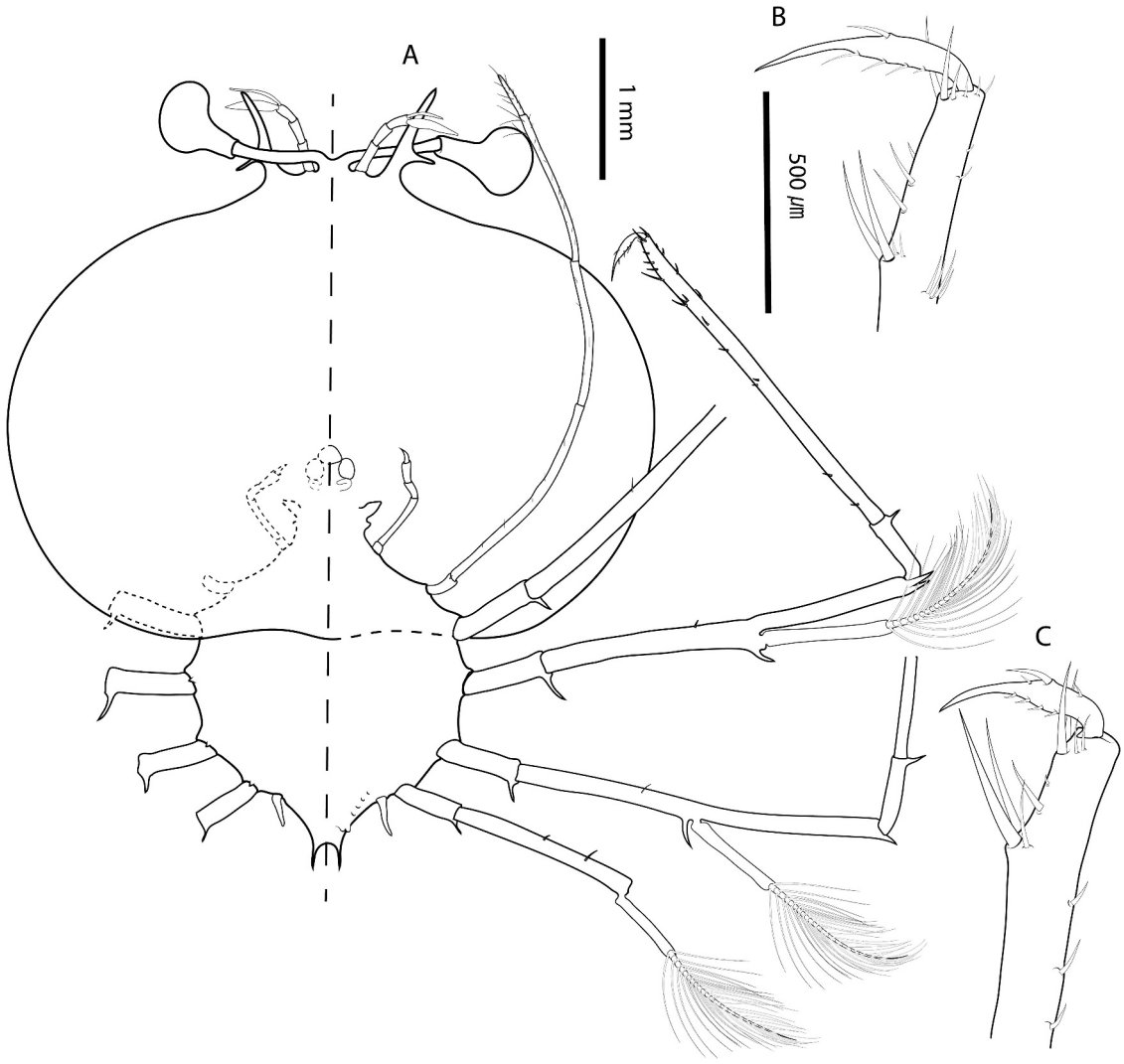

Figure 3. *Chelarctus aureus* (Holthuis, 1963), stage VI. A, ventral (right) and dorsal (left) view; B, dactylus of second pereiopod; C, dactylus of third pereiopod. Scale bars: A = 1 mm; B and C = 500 µm.

Chelarctus aureus and *Ch. crosnieri* phyllosomae are reported from Western Coral Sea waters for the first time, and *Chelarctus* adults were never recorded here before (Figure 2). Intermediate (stage VI), subfinal (IX) and final (X) stages of *Ch. aureus* and subfinal (IX) and final (X) stages for *Ch. crosnieri* are described in detail (Figures 3–12). The subfinal stage of *Ch. crosnieri* was identified by the number of spines in maxillae and maxillipeds, number of aesthetascs and BL. Specimens identified as *Cr. crenatus* (MNHN-IU-2017-2420 and MNHN-IU-2017-10,460) or *Ch. virgosus* (NMNS-004987-00006) are not redescribed here because they are identical to those accurately drawn by Webber and Booth (2001) and Johnson (1979), but *Chelarctus* and *Crenarctus* larval morphology is compared in Table II. Cephalon shape, Crp/Prd ratio of maxilliped 3 and P5 articulation allow to differentiate both genera, while morphometrics (CL/CW, BL/CW, PL/PW) of final stage phyllosoma define two groups: *Ch. aureus*/*Ch. crosnieri* and *Ch. virgosus*/Chelarctus sp.1/*Crenarctus*.

Chelarctus aureus **(Holthuis, 1963)**

Stage VI (*samples from cruise C5160: 26_03, 15_02, 50_02, 50_03*). *Morphometrics*: N = 6, BL = 8.9–10.5 mm, CL = 6.7–7.2 mm, CW = 8.8–9.7 mm, TL = 3.3–3.7 mm, TW = 3.6–3.8 mm, PL = 0.7–0.8 mm, PW = 1.2–1.3 mm, CL/CW = 0.8–0.7. *Cephalic shield* (Figure 3A): Rectangular shape, wider than longer. *Antennule* (Figures 3A, 4A) equal in length than antenna, with 3-articulated

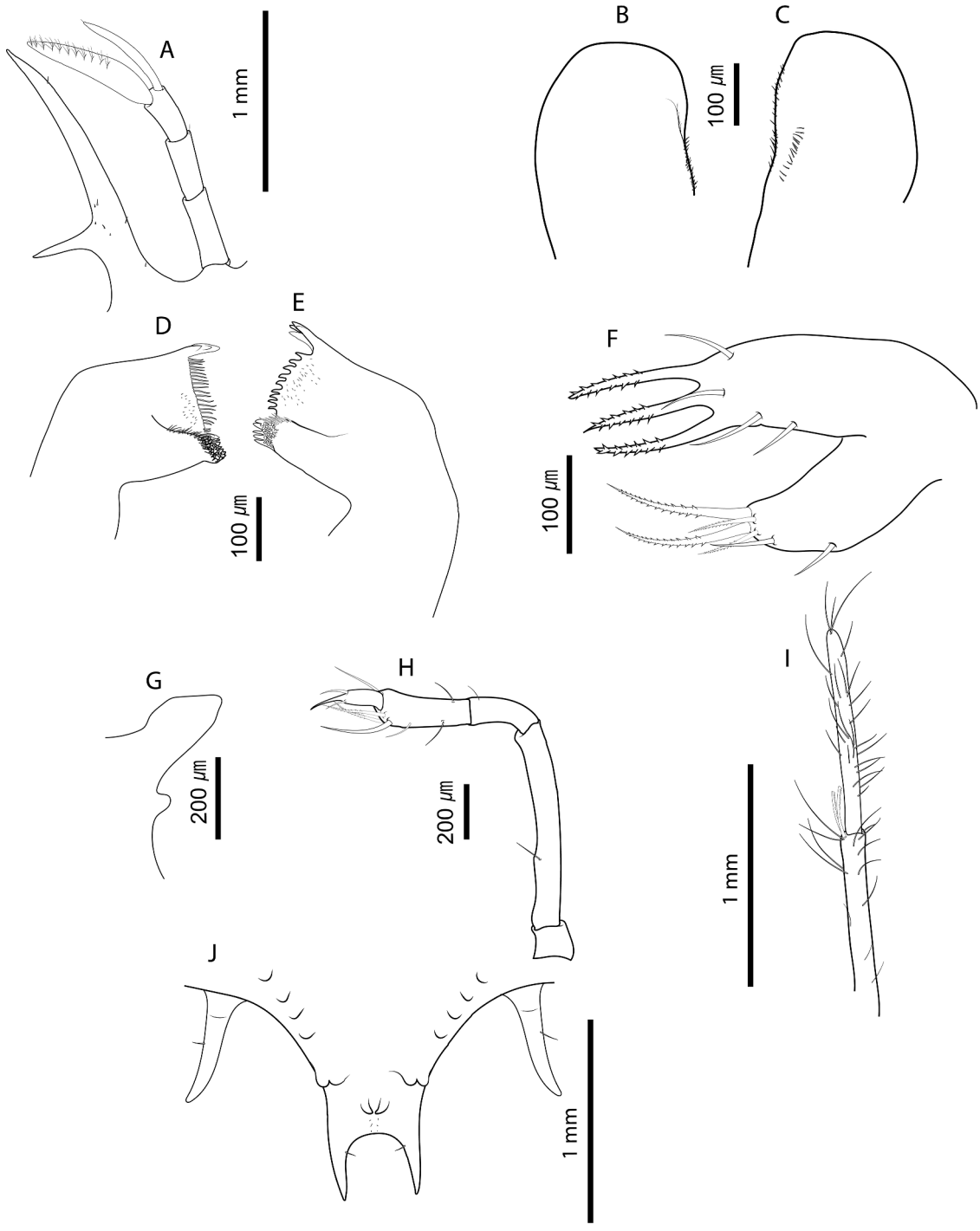

Figure 4. *Chelarctus aureus* (Holthuis, 1963), stage VI. A, antenna and antennule; B, C, left and right paragnaths (ventral view); D, E, left and right mandibles (dorsal view); F, maxillule; G, maxilla and first maxilliped; H, second maxilliped; I, third maxilliped (distal part); J, pleon and fifth pereiopod (ventral view). Scale bars: A, J and I = 1 m; B–F = 100 µm; G, H = 200 µm.

peduncle. Primary flagellum with 10–11 rows of aesthetascs; accessory flagellum shorter than primary. *Antenna* (Figures 3A, 4A): Biramous, unarticulated, shorter than antennule; endopod longer than exopod. *Paragnaths* (Figure 4B, C): Asymmetrical. Both fringed marginally with setules and denticulettes. *Mandibles* (Figure 4D, E): Asymmetrical dentition. Both mandibles with abundant small teeth distributed over surface and molar process crowned with many denticles. Left mandible

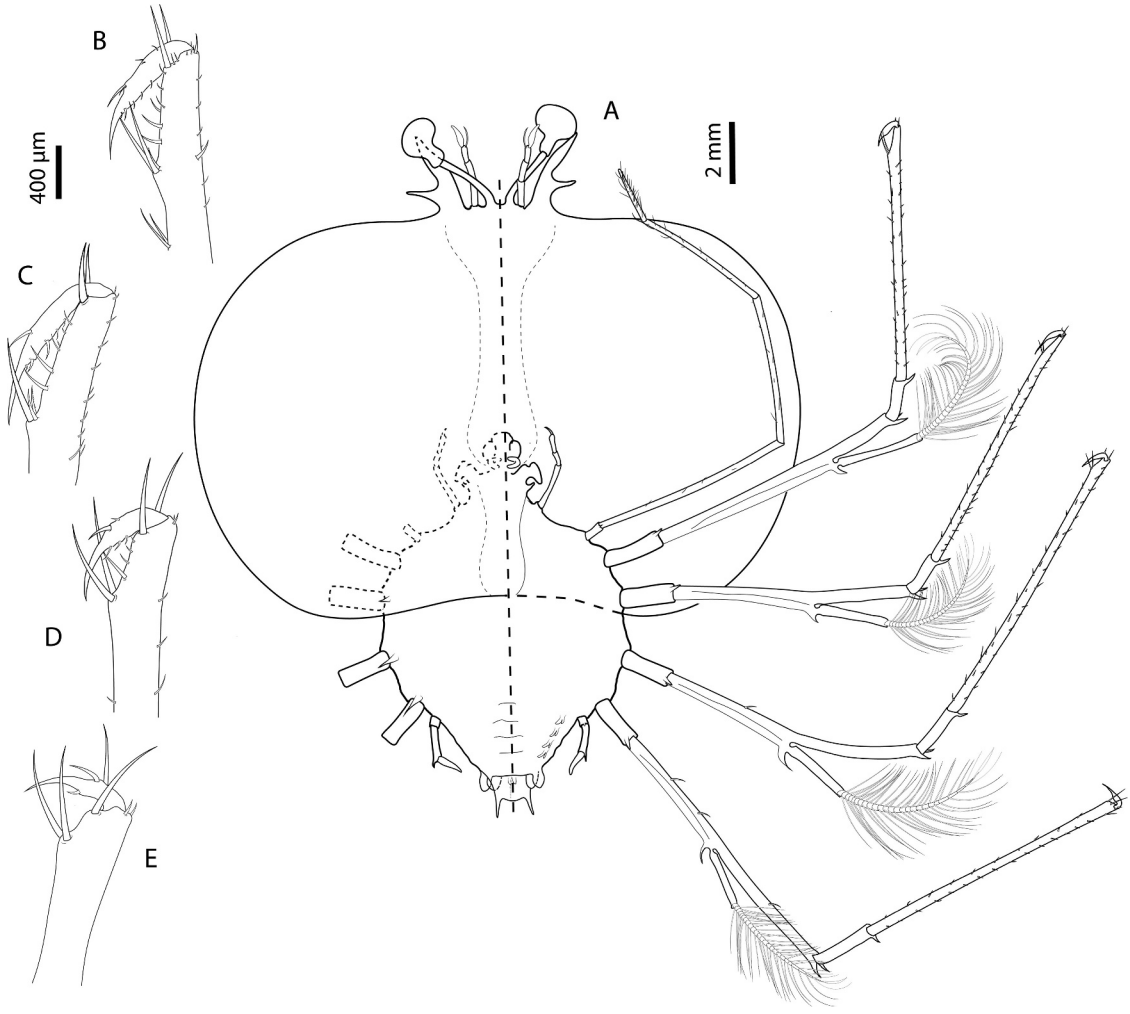

Figure 5. *Chelarctus aureus* (Holthuis, 1963), subfinal stage. A, ventral (right) and dorsal (left) view; B, dactylus of first pereiopod; C, dactylus of second pereiopod; D, dactylus of third pereiopod; E, dactylus of fourth pereiopod. Scale bars: A = 2 mm; B–E = 400 µm.

with 3 elongated teeth on incisor process; right mandible with 4 teeth curved towards molar process. Palp absent. *Maxillule* (Figure 4F): Coxal endite with 2 simple setae and 4 serrate setae (2 long and strong); basial endite with 4 simple setae and 3 cuspidate setae with denticles, long and strong. Endopod and exopod absent. *Maxilla* (Figures 3A, 4G): Unarticulated and underdeveloped. *First maxilliped* (Figures 3A, 4G): Present as minute bud. *Second maxilliped* (Figures 3A, 4H): Uniramous. Coxa without setae; basis delimited by distal seta; endopod with 4 articles, ischium-merus (undifferentiated), carpus, propodus and dactylus with 1, 0, 7 (2 serrate setae) and 2 setae, respectively. Exopod absent. *Third maxilliped* (Figures 3A, 4I): Uniramous. Coxa with ventral distal spine; basis and endopod undifferentiated; endopod with 4 articles, ischium-merus (undifferentiated), carpus, propodus and dactylus with 5, 6, 23 (2 distal serrate) and ~30 simple setae, respectively. Setae on inner margin longer than outer margin. Exopod absent. *Pereiopods* (Figures 4A–C, 4J): P1–4 biramous. Coxa without setae, long distal ventral spine; basis delimited by distal spine, P1–3 basis with medial seta, P4 basis with 2 medial setae; endopod 4-articulated, ischium-merus (undifferentiated) with 2 distal spines, carpus with distal spine. Dactylus of P2 and P3 with 5 and 7 simple setae, respectively. P1–4 exopods with 19, 19–21, 18–19, 17 annulations respectively, each annulation with 2 long plumose setae. P5 (Figure 4J) uniramous and unarticulated with minute seta. Exopod absent. *Thorax* (Figure 3A): Sternites 5–7 with dorsal distal spine. Sternite 4 and 8 without spine. *Pleon* (Figures 3A, 4J): Pleopod 1 absent. Pleopods 2–5 uniramous, not developed, endopod present, exopod absent.

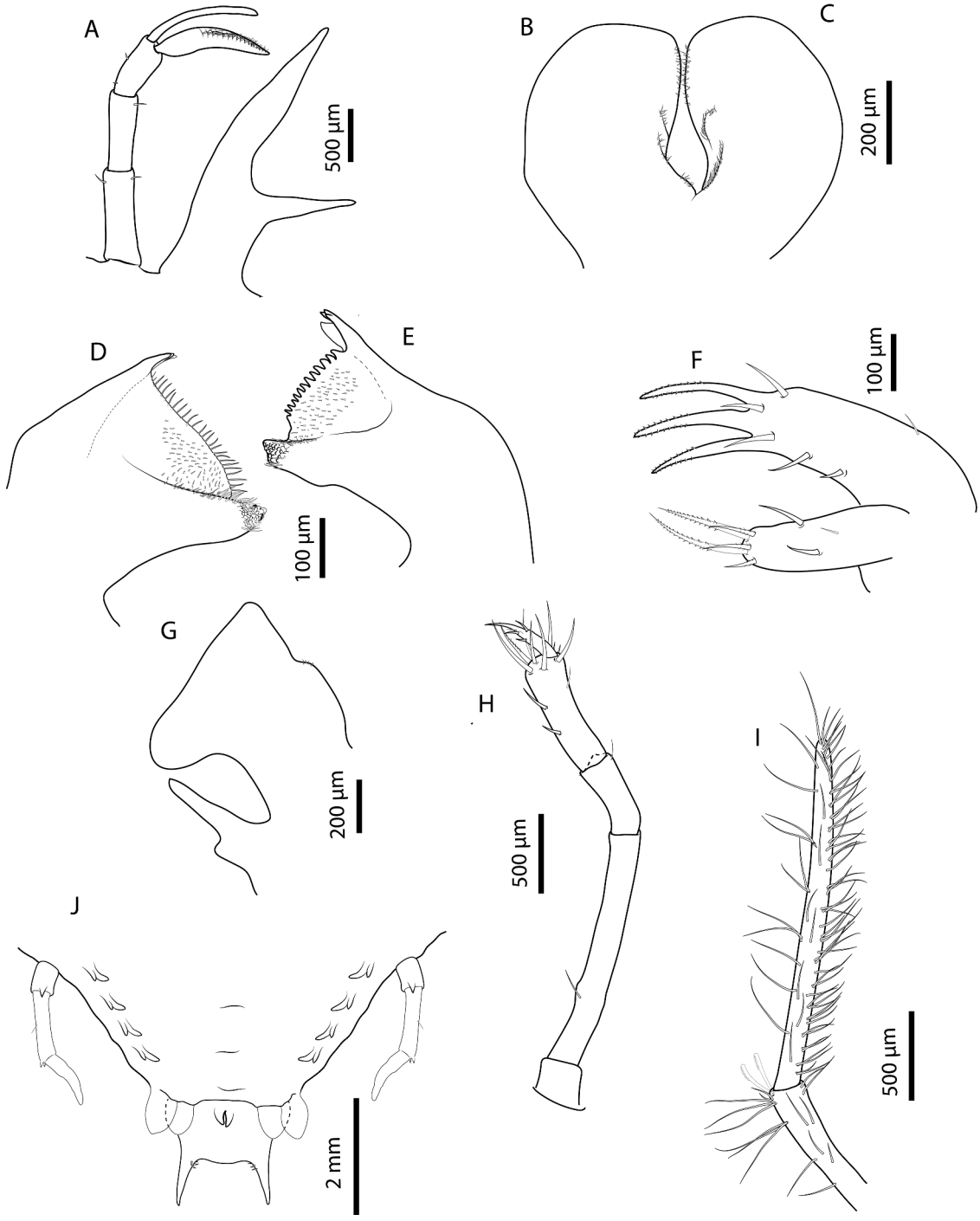

Figure 6. *Chelarctus aureus* (Holthuis, 1963), subfinal stage. A, antenna and antennule; B, C, left and right paragnaths (ventral view); D, E, left and right mandibles (dorsal view); F, maxillule; G, maxilla and first maxilliped; H, second maxilliped; I, third maxilliped (distal part); J, pleon and fifth pereiopod (ventral view). Scale bars: A, H and I = 500 µm; B, C and G = 200 µm; D–F = 100 µm; J = 2 mm.

Uropods biramous. *Telson* (Figures 3A, 4J): Margin concave, 2–3 pairs of dorsal setae, 2 long terminal processes with proximal seta each.

Stage IX (C5441: 142_01, 142_02, 205_02, 175_01)

Morphometrics: N = 4, BL = 16.9–19.7 mm, CL = 11.1–12.9 mm, CW = 16.6–19.8 mm, TL = 6.0–9.8 mm, TW = 6.8–8.2 mm, PL = 1.9–2.6 mm, PW = 3.6–4.4 mm, CL/CW = 0.65–0.67. *Cephalic shield* (Figure 5A): Rectangular shape, wider than longer. *Antennule* (Figures 5A, 6A): Primary flagellum with 16–17 rows of aesthetascs. Simple setae in both margins of antennular

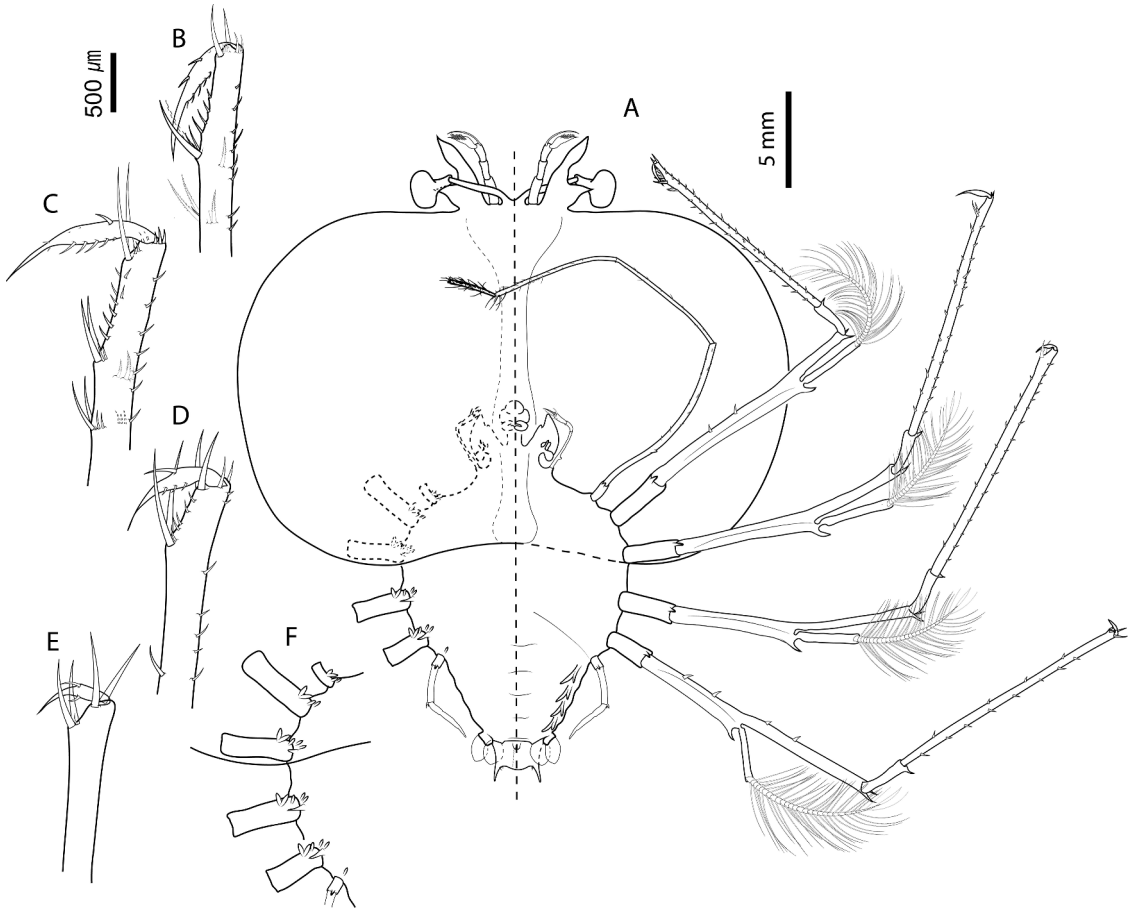

Figure 7. *Chelarctus aureus* (Holthuis, 1963), final stage. A, ventral (right) and dorsal (left) view; B, dactylus of first pereiopod; C, dactylus of second pereiopod; D, dactylus of third pereiopod; E, dactylus of fourth pereiopod. Scale bars: A = 5 mm; B–E = 500 µm.

peduncle. *Antenna* (Figures 5A, 6A): equal in length than antennule. *Paragnaths* (Figure 6B, C): Both with more setae than previous stage. Otherwise unchanged. *Mandibles* (Figure 6D, E): Both mandibles with more teeth than previous stage. Otherwise unchanged. *Maxillule* (Figures 5A, 6F): Coxal endite with 3 simple setae and 5 serrate setae (2 long and strong); basial endite with 5 simple setae and 3 cuspidate setae with denticles, long and strong. Otherwise unchanged. *Maxilla* (Figures 5A, 6G): Uniramous and unarticulated. Endites and endopod not differentiated with 4–5 setae on superior margin; scaphognathite (exopod) present, slightly developed and rectangular, without marginal setae. *First maxilliped* (Figures 5A, 6G): Uniramous. Endites undifferentiated; endopod present and unarticulated. Exopod absent. *Second maxilliped* (Figures 5A, 6H): Endopod 4-articled, ischium-merus (undifferentiated), carpus, propodus, dactylus with 0, 1, 12 (1 serrate seta) and 4 simple setae respectively. Otherwise unchanged. *Third maxilliped* (Figures 5A, 6I): Endopod 4-articled, ischium-merus (undifferentiated), carpus, propodus and dactylus with ~8, ~10, ~40 (2 distal serrated) and ~70 simple setae respectively. Setae on inner margin longer than outer margin. Otherwise unchanged. *Pereiopods* (Figures 5A-E, 6J): P1–4 biramous. Coxa without setae, distal ventral spine present; basis delimited by distal spine, P1–P2 without medial spines, P3 with medial spine, P4 with 2 medial spines; endopod 4-articled, ischium-merus (undifferentiated) with 2 distal spines, carpus withdistal spine, propodus with 75, 50, 50 and 25 small simple setae scattered over article surface, dactylus with 10, 6, 5, 2 setae respectively. Exopod with 25, 25–27, (> 21)–26, (> 20)–26 annulations respectively. P5 (Figure 6J) Uniramous. Coxa without setae, ventral distal spine present; basis delimited by medial spine; endopod 2-articled, ischium-merus (undifferentiated) with 2 distal spines, proximal articles not differentiated. Exopod absent. *Thorax* (Figure 5A): Dorsal distal spine larger than previous. Otherwise unchanged. *Pleon* (Figures 5A, 6J) Pleopod 1 absent. Pleopods 2–5 and uropods biramous.

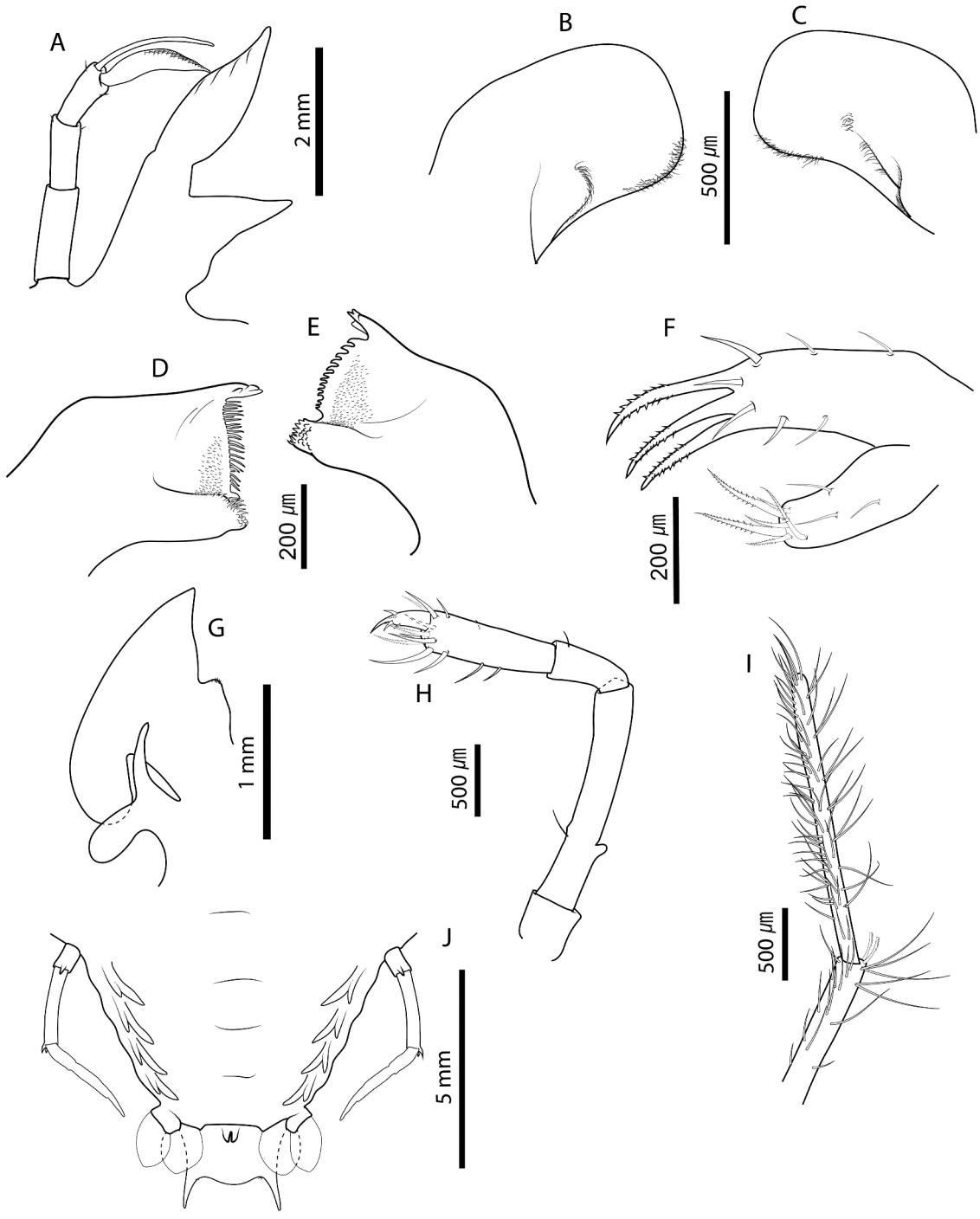

Figure 8. *Chelarctus aureus* (Holthuis, 1963), final stage. A, antenna and antennule; B, C, right and left paragnaths (ventral view); D, E, left and right mandibles (dorsal view); F, maxillule; G, maxilla and first maxilliped; H, second maxilliped; I, third maxilliped (distal part); J, pleon and fifth pereiopod (ventral view). Scale bars: A = 2 mm; C, D, H and I = 500 µm; D–F = 200 µm; G = 1 mm; J = 5 mm.

Telson (Figures 5A, 6J): Fork margin slightly concave, proximal setae on inner margin probably missing, 6–8 pairs of dorsal setae.

Stage X (C5160: 413_01; C5441: 68_01, 205_04, 214_01, 214_04) Morphometrics: N = 5, BL = 21.6–24.3 mm, CL = 13.2–14.7 mm, CW = 20.5–22.8 mm, TL = 7.4–8.5 mm, TW = 8.9–10.3 mm, PL = 3.9–4.5 mm, PW = 5.4–6.3 mm, CL/CW = 0.63–0.65. *Cephalic shield* (Figure 7A): Unchanged. *Antennule* (Figures 7A, 8A): Slightly shorter than antenna. Primary flagellum with 17–18 rows of sensory setae, accessory flagellum

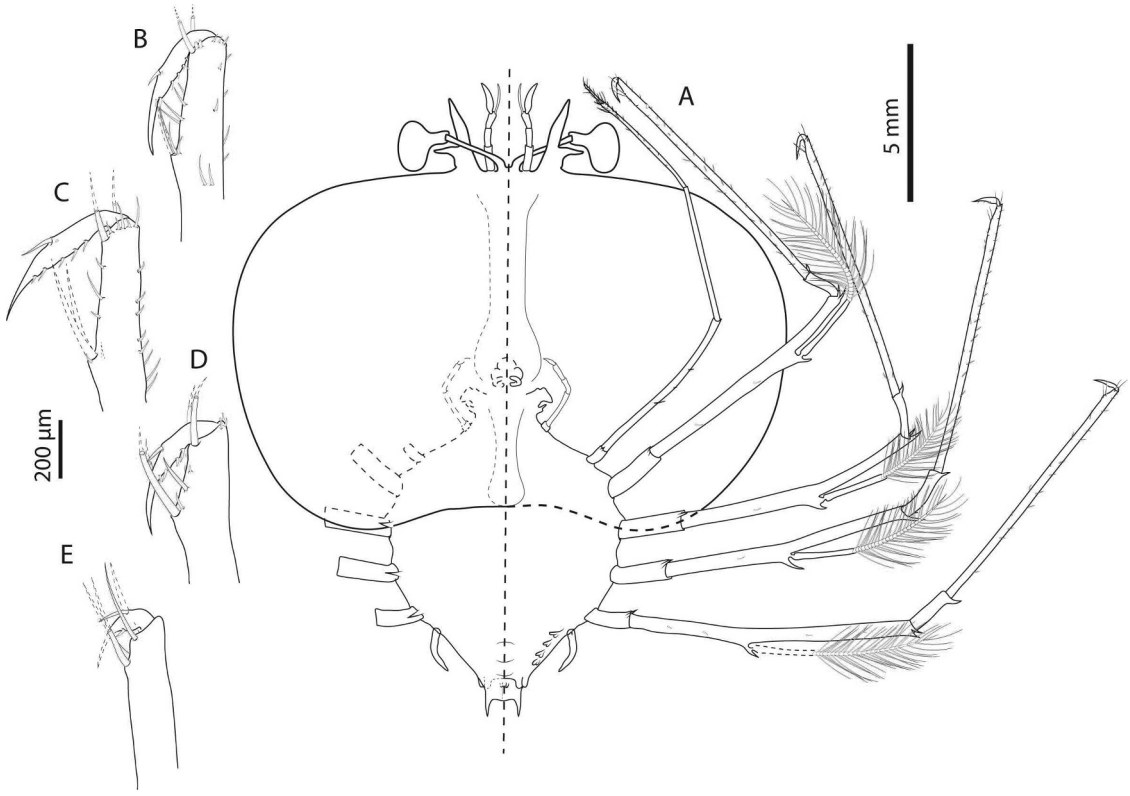

Figure 9. *Chelarctus crosnieri* Holthuis, 2002, subfinal stage. A, ventral (right) and dorsal (left) view; B, dactylus of first pereiopod (P1); C, dactylus of second pereiopod; D, dactylus of third pereiopod (P3); E, dactylus of fourth pereiopod (P4). Scale bars: A = 5 mm; B–E = 200 µm.

unarticled with minute setae in both margins. *Antenna* (Figures 7A, 8A): Slightly longer than antennule, with perceptible lobular articulation. *Paragnaths* (Figure 8B, C): Unchanged. *Mandibles* (Figure 8D, E): Both mandibles with more teeth than previous stage. Left mandible with 4 teeth on incisor process. Palp absent. *Maxillule* (Figures 7A, 8F): Coxal endite with 6 serrate setae and 3 simple setae; basial endite with 3 cuspidate setae with denticles and 7 simple setae. Otherwise unchanged. *Maxilla* (Figures 7A, 8G): Uniramous. Endite and endopod undifferentiated with 5–6 setae on superior margin of lateral process; scaphognathite (exopod) flattened and expanded, without marginal setae. *First maxilliped* (Figures 7A, 8G): Unarticulated and bilobed; outer lobe (endite) flattened and round; inner lobe (endopod) elongated and unarticulated. Exopod absent. *Second maxilliped* (Figures 7A, 8H): Biramous. Coxa without setae; basis delimited by distal seta; endopod with 4 articles, ischium-merus (undifferentiated), carpus, propodus, dactylus with 0, 1, 13 (2 serrate setae) and simple 5 setae respectively. Exopod present as minute bud. *Third maxilliped* (Figures 7A, 8I): Biramous. Gills buds present; 1 pleurobranch, 1 arthrobranch and 2 podobranchs. More densely setose than previous stage. Basis delimited by exopod (minute bud); endopod with 4 articles, ischium-merus (undifferentiated), carpus, propodus and dactylus with 10, 8, 50 (2 distally serrated) and ~100 simple setae respectively. Otherwise unchanged. *Pereiopods* (Figures 7A–E, 8J): P1–4 biramous. P1–P4 basis with 2 medial setae, P2–P3 setae probably missing; propodus with 85, 65, 40 and 25 small simple setae scattered over the surface, dactylus with 8, 10, 4, 2 simple setae respectively. Exopods with 23–27, 23–26, 25–27 and 23–25 annulations respectively. Otherwise unchanged. P5 longer than previous stage. *Gills* (Figure 7A, F): Gill buds present. P1 with 1 pleurobranch, 1 arthrobranch and 2 podobranchs. P2–P4 with 2 pleurobranchs, 1 arthrobranch, 2 podobranchs. P5 with 1 pleurobranch. *Thorax* (Figure 7A, F): Unchanged. *Pleon* (Figures 7A, 8J): Pleopods and uropods well-developed. *Telson* (Figures 7A, 8J): 9–11 paired dorsal setae. 2 long terminal processes with 1 pair of setae each in inner margin.

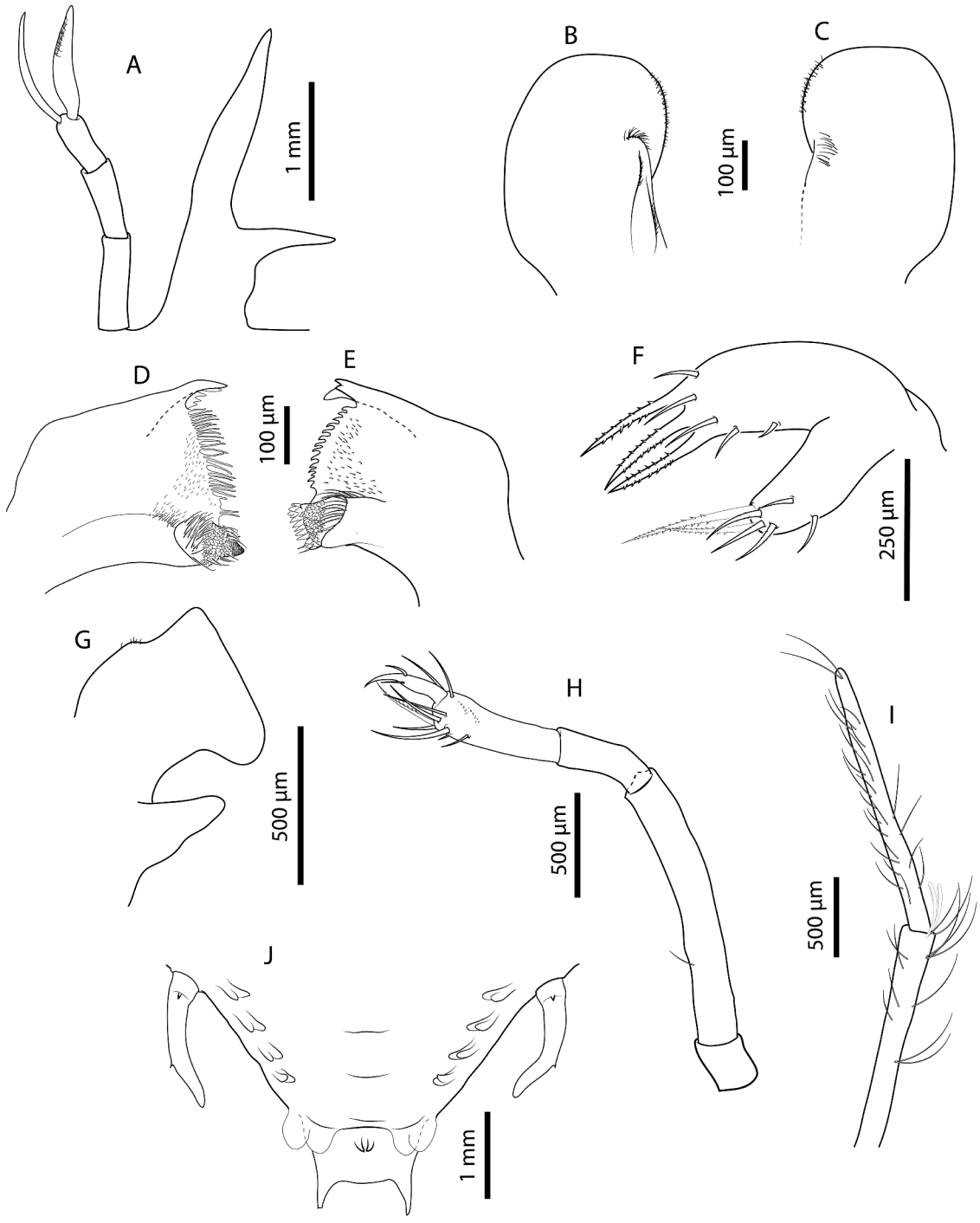

Figure 10. *Chelarctus crosnieri* Holthuis, 2002, subfinal stage. A, antenna and antennule; B, C, left and right paragnaths (ventral view); D, E, left and right mandibles (dorsal view); F, maxillule; G, maxilla and first maxilliped; H, second maxilliped; I, third maxilliped (distal part); J, pleon and fifth pereiopod (ventral view). Scale bars: A and J = 1 mm; B–D = 100 µm; F = 250 µm; G–I = 500 µm.

Chelarctus crosnieri **Holthuis, 2002**

Stage IX (C5441: 159_02, 205_08, 205_10, 205_11) Morphometrics: N = 5, BL = 13.1–17.5 mm, CL = 10.3–11.7 mm, CW = 16.4–16.7 mm, TL = 5.7–6.1 mm, TW = 6.6–7.0 mm, PL = 1.9–2.3 mm, PW = 3.5–4.0 mm, CL/CW = 0.67–0.70. *Cephalic shield* (Figure 9A): Rectangular shape, wider than longer. *Antennule* (Figures 9A, 10A): Slightly longer than antenna with 3-articled peduncle. Primary flagellum with 11 rows of aesthetascs; accessory flagellum equal in length than primary.

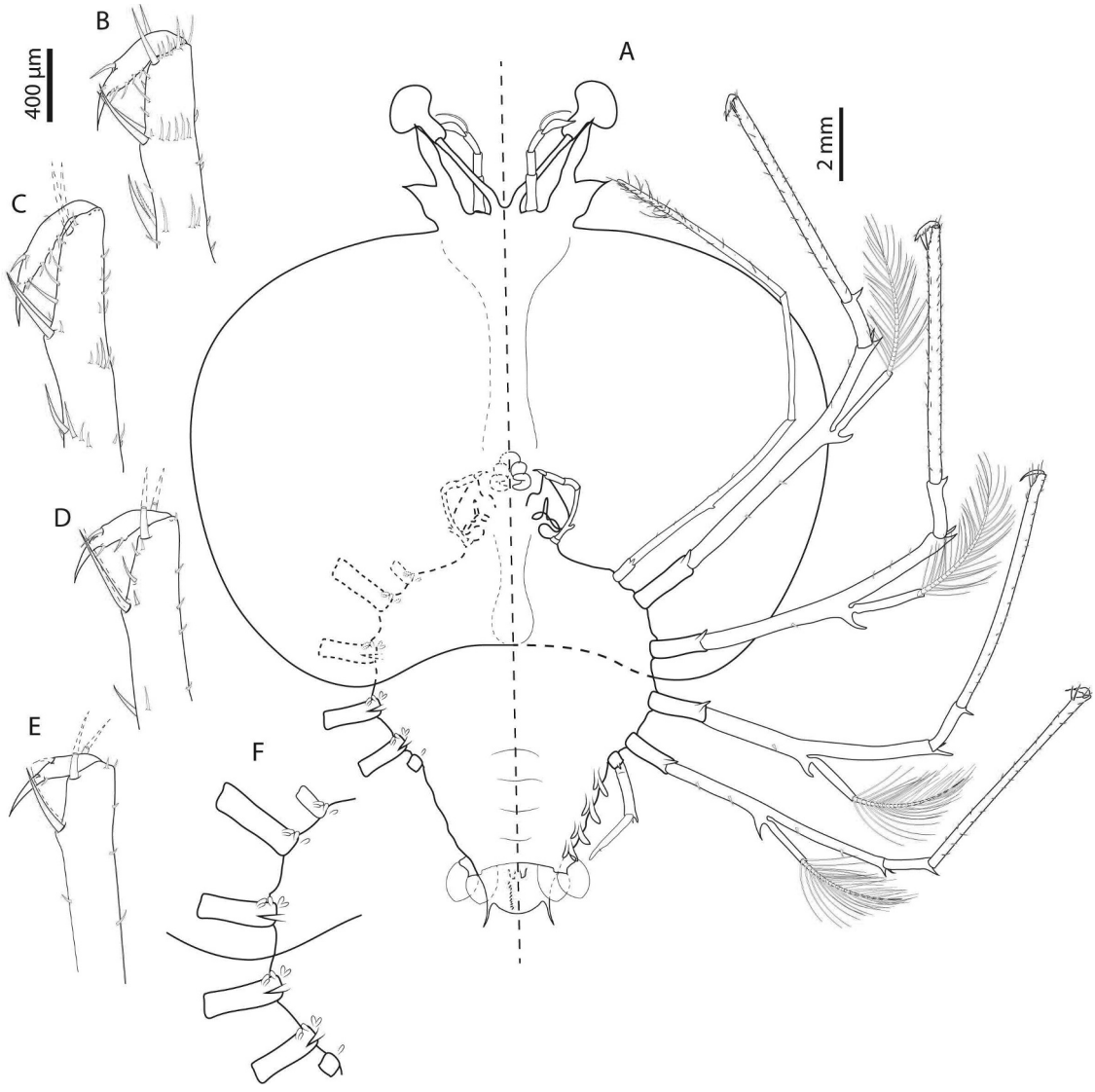

Figure 11. *Chelarctus crosnieri* Holthuis, 2002, final stage. A, ventral (right) and dorsal (left) view; B, dactylus of first pereiopod (P1); C, dactylus of second pereiopod (P2); D, dactylus of third pereiopod (P3); E, dactylus of fourth pereiopod (P4). Scale bars: A = 2 mm; B–E = 400 µm.

Antenna (Figures 9A, 10A): Biramous. Not articulated, slightly shorter than antennule. *Paragnaths* (Figure 10B, C): Asymmetrical. Both with fringed marginally with setules and denticulettes. *Mandibles* (Figure 10D, E): Asymmetrical dentition. Both mandibles with abundant small teeth distributed over surface and molar process crowned with many different denticles. Left mandible with multiple teeth on incisor process, right mandible larger and with 3 teeth on incisor process; right mandible teeth curved towards molar process while teeth of right mandible are elongated. Palp absent. *Maxillule* (Figures 8A, 10F): Coxal endite with 5 serrate setae (2 long and strong) and 2 simple setae; basial endite with 3 cuspidate setae with denticles, long and strong and 5 simple setae. Endopod and exopod absent. *Maxilla* (Figures 9A, 10G): Uniramous and unarticulated. Endites and endopod undifferentiated with 5 simple setae on superior margin; scaphognathite (exopod) slightly developed and rectangular, without marginal setae. *First maxilliped* (Figures 9A, 10G): Present and undifferentiated. *Second maxilliped* (Figures 9A, 10H): Uniramous. Coxa without setae; basis delimited by distal simple seta; endopod with 4 articles, ischium-merus (undifferentiated), carpus, propodus (elongated) and dactylus with 0, 0, 11 (2 serrate setae) and 3 simple setae respectively. Exopod absent. *Third maxilliped* (Figures 9A, 10I): Uniramous. Coxa without setae, ventral spine present; basis not differentiated,

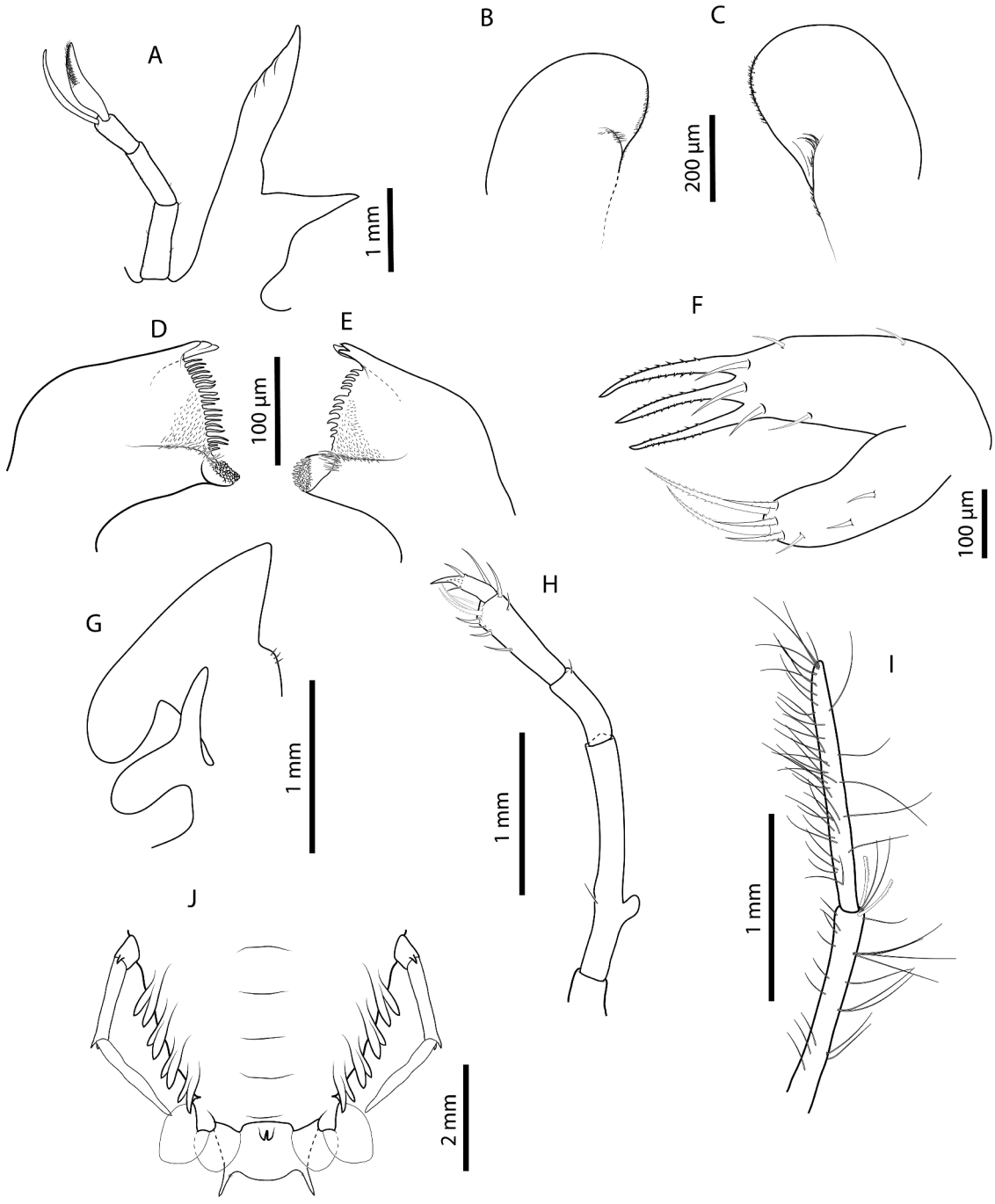

Figure 12. *Chelarctus crosnieri* Holthuis, 2002, final stage. A, antenna and antennule; B, C, right and left paragnaths (ventral view); D, E, left and right mandibles (dorsal view); F, maxillule; G, maxilla and first maxilliped; H, second maxilliped; I, third maxilliped (distal part); J, pleon and fifth pereiopod (ventral view). Scale bars: A, G–I = 1 mm; B and C = 200 µm; D–F = 100 µm.

without setae; endopod 4-articled, ischium-merus (undifferentiated), carpus, propodus and dactylus with 3, 0, 33 (2 distal serrate setae) and 70 simple setae respectively. Setae on inner margin longer than outer margin. Exopod absent. *Pereiopods* (Figures 9A–E, 10J): P1–4 biramous. Coxa without setae and with distal ventral spine; basis elongated and demarcated distally by single spine; endopod 4-articled, ischium-merus (undifferentiated) with two distal spines, carpus with one distal spine, propodus with 60, 55, 40 and 25 simple setae scattered over article surface, dactylus with 8, 7, 5 and 2 simple setae respectively. Exopod with (>20) –25, (>14)–26, 24–25, 21–25 annulations respectively, each annulation with two long plumose setae. P5 (Figure 10J) Uniramous. Coxa with ventral distal

spine; basis demarcated by single spine; endopod with article, proximal articles undifferentiated. Exopod absent. *Thorax* (Figure 9A): Sternites 5–7 with dorsal distal spine. Sternite 4 and 8 without spine. *Pleon* (Figures 9A, 10J): Pleopod 1 absent, pleopods 2–5 and uropods biramous. *Telson* (Figures 9A, 10J): Margin slightly concave with 2 terminal processes proximally.

Stage X (C5441: 159_01, 181_01, 181_02, 181_03, 205_01, 205_06) Morphometrics: N = 6, BL = 17.7–19.2 mm, CL = 10.7–11.7 mm, CW = 14.6–16.3 mm, TL = 5.5–5.9 mm, TW = 6.8–7.4 mm, PL = 3.7–4.0 mm, PW = 4.5–5.0 mm, CL/CW = 0.70–0.74. *Cephalic shield* (Figure 11A): Unchanged. *Antennule* (Figures 11A, 12A): Slightly shorter than antenna. Accessory flagellum unarticulated; primary flagellum slightly shorter than accessory with 15–16 rows of sensory setae. *Antenna* (Figures 11A, 12A): With perceptible lobular articulation. *Paragnaths* (Figure 12B, C): Unchanged (right paragnath damaged). *Mandibles* (Figure 12D, E): More teeth in both mandibles than previous stage. Otherwise unchanged. *Maxillule* (Figure 12F): Coxal endite with 5 serrate and 3 simple setae; basial endite with 3 cuspidate setae with denticles and 6 simple setae. Otherwise unchanged. *Maxilla* (Figures 11A, 12G): Uniramous. Endites and endopod not differentiated with 3–4 simple setae on lateral process; scaphognathite (exopod) flattened and expanded, without marginal setae. *First maxilliped* (Figures 11A, 12G): Uniramous and bilobed. Endite flattened, rounded, not differentiated. Endopod elongated and unarticulated. Exopod absent. *Second maxilliped* (Figures 11A, 12H): Biramous. Coxa without setae; basis delimited by distal setae; endopod present with 4 articles, ischium-merus (undifferentiated), carpus, propodus and dactylus with 0, 1, 10 (3 serrate setae) and 3 simple setae, respectively. Exopod present as minute bud. *Third maxilliped* (Figures 11A, 12I): Biramous. Gill buds present; 1 pleurobranch, 1 arthrobranch and 2 podobranchs. More densely setose than previous stage. Basis delimited by exopod (minute bud); endopod, propodus and dactylus with 35 (2 distal serrate setae) and > 60 simple setae, respectively. Otherwise unchanged. *Pereiopods* (Figures 11A–E, 12J): P1–4 biramous. Propodus with 75, 60, 40 and 20 small simple setae scattered over the surface, dactylus with 8, 10, 4 and 4 respectively. Exopods with 23–25, 23–26, 25–27 and 23–25 annulations respectively. Otherwise unchanged. P5 (Figure 12J) basis and ischium-merus not differentiated (probably seta on basis missing); endopod with 2 articles, ischium-merus with two distal spines, proximal articles undifferentiated. Longer than previous stage. *Gills* (Figure 11A, F): Gill buds present; P1 with 1 pleurobranch, 1 arthrobranch and 2 podobranchs; P2–P4 with 2 pleurobranchs, 1 arthrobranch, 2 podobranchs; P5 with 1 pleurobranch. *Thorax* (Figure 11A, F): Unchanged. *Pleon* (Figures 11A, 12J): Pleopods and uropods biramous and well-developed. *Telson* (Figures 11A, 12J): 9–11 paired setae dorsally. Otherwise unchanged.

Discussion

Final larval stages of *Chelarctus crosnieri* and *Crenarctus crenatus* are identified by DNA barcoding for the first time, as well as larval stages VI, IX and X of *Chelarctus aureus*. These results, together with a thorough revision of the previous literature, allowed *Chelarctus* and *Crenarctus* subfinal and final stages to be distinguished based on cephalic shield shape, relative length of carpus and propodus of maxilliped 3 (Crp/Prd ratio) and P5 articulation in the final larval stage. *Chelarctus* phyllosomae present a kidney-shape cephalon with a convex posterior margin, while *Crenarctus* show a rectangular cephalon shape with straight margin. Similarly, *Chelarctus* phyllosomae show a significantly larger Crp/Prd ratio (≥ 0.9) than *Crenarctus* specimens (≤ 0.7). Regarding P5 articulation in the last stage, *Crenarctus* larvae have 4-articled P5, whereas P5 in *Chelarctus* has only three articles. The presence of 4-articles mentioned by some authors (Higa & Shokita 2004; Inoue & Sekiguchi 2006; Ueda et al. 2021) is contradicted by previous works on North Pacific larvae (Johnson 1971, 1979; Sekiguchi 1990) and our results. This oversight is probably due to the apparent swelling, but lack of segmentation, of the P5 of *Chelarctus* final stage phyllosomae. The number of antennular sensory setae or spines on maxillipeds and pereiopods also seem to be useful characters to distinguish *Ch. aureus* and *Ch. crosnieri* larvae. The characters suggested to distinguish *Ch. aureus* larvae by Ueda et al. (2021) were based on single specimens for each stage and do not hold when the new Coral Sea phyllosomae are considered. The larval description of *Chelarctus* sp., assigned by the same authors to a putative *Ch. crosnieri* subspecies, is limited and should be examined accurately to discard the presence of pseudogenes and gather further morphological evidence.

Crenarctus crenatus and *Ch. virgosus* larvae have been confused in the literature until recently (Webber & Booth 2001; Ueda et al. 2021) because both share morphological characters such as BL or

narrow cephalon and pleon. New molecular results and detailed morphological analyses using trait differences that had previously passed unnoticed (e.g., length of carpus and propodus of maxilliped 3), have allowed us to re-assess inferences made by previous authors. Our results support that the larval series *Scyllarus* sp. Z, tentatively assigned to *S. aoteanus* by Webber and Booth (2001), belongs to *Cr. crenatus*. Indeed, *S. aoteanus* was recently synonymized with *Cr. crenatus* by Chan et al. (2013). Likewise, the morphology of *S. delfini* phyllosomae (see Baez 1973) is very similar to our *Cr. crenatus* larvae (Table II) and specimens from Juan Fernández island (Palma et al. 2011) cluster with *Cr. crenatus* and *Cr. bicuspidatus*. These results are congruent with previous observations of adult morphology and confirm that *Acantharctus delfini* should be considered as *Cr. delfini* (Genis-Armero et al. 2020). The taxonomy of *Acantharctus* and, more generally, the Scyllarinae, need a thorough revision using both morphological and molecular data.

Previous phylogeographic studies have uncovered complexes of cryptic species on shallow-water taxa from West Pacific (shrimps: Tsoi et al. 2007; cephalopods: Cheng et al. 2014; bivalves: DeBoer et al. 2014). While COI has been generally used as supporting evidence for establishing new taxa (Poore & Andreakis 2011; Tsoi et al. 2011), identifying new species with one gene can be misleading (Ballard & Whitlock 2004; Galtier et al. 2009) and might overestimate biodiversity (Song et al. 2008). Despite COI genetic distances were higher, a second mitochondrial gene (16S) and the nuclear marker (18S) did not show any intraspecific variation between Coral Sea *Chelarctus* larvae and their putative adults (*Ch. aureus*/*Ch. crosnieri*). Moreover, the significantly higher intraspecific variation observed for *Ch. aureus* when using COI primers designed by Folmer et al. (1994) suggest the presence of nuclear mitochondrial pseudogenes, which have already been found in several crustaceans (Buhay 2009) and particularly in decapods (Williams & Knowlton 2001; Nguyen et al. 2002; Schubart 2009). The new pair of primers proposed by Krehenwinkel et al. (2018), designed specifically to amplify arthropod DNA, seem to be a better option when analyzing crustacean taxa. Although COI has been popularized as the main DNA barcoding gene, it may provide misleading results and it should be complemented with evidence from other mitochondrial and nuclear genes. The new evidence presented here highlight the value of integrative studies, combining comprehensive molecular data with detailed morphological analyses from adults and larvae. A particular focus should be given to increase the number of markers and to further explore Southern Hemisphere populations to better understand phylogeography and diversity of lobsters along the IWP.

Acknowledgements

This paper is dedicated to the late Alain Crosnier, for his invaluable work in advancing carcinology. Thanks are due to Dr. Hall for shipping the larvae and the crew of the Research Vessel *Cape Ferguson* and staff and volunteers on the collection trips and the Australian Institute of Marine Science for ship time. We also thank Laure Corbari and Paula Martin-Lefevre (Muséum national d'Histoire naturelle, Paris) and Romana Capaccioni and her team (Marine Biology Lab, University of Valencia) for encouraging the completion of this work. FP acknowledges the projects "CIDEGENT/2019/028 - BIOdiversity PAtterns of Crustacea from Karstic Systems (BIOPACKS): molecular, morphological, and functional adaptations" funded by the Conselleria d'Innovació, Universitats, Ciència i Societat Digital and "PRO2020-S02-PALERO - Fauna aquàtica en coves anquihalines del País Valencià: un mon encara per descriure" funded by the Institut d'Estudis Catalans.

Funding

This work was supported by the EU-Synthesys grant GB-TAF-2737: DNA barcoding identification of phyllosoma larvae from Coral Sea waters; FP acknowledges the projects "CIDEGENT/2019/028 - BIOdiversity PAtterns of Crustacea from Karstic Systems (BIOPACKS): molecular, morphological, and functional adaptations" funded by the Conselleria d'Innovació, Universitats, Ciència i Societat Digital and "PRO2021-S02-PALERO - Fauna aquàtica en coves anquihalines del País Valencià: un mon encara per descriure" funded by the Institut d'Estudis Catalans. The research was financed by NCN OPUS BIOPASS 2018/31/B/NZ8/03198."

Disclosure statement

No potential conflict of interest was reported by the author(s).

Sampling and field studies

All necessary permits for sampling and observational field studies have been obtained by the authors from the competent authorities and are mentioned in the acknowledgements.

Supplemntal material

Supplemental data for this article can be accessed here

ORCID

R. Genis-Armero http://orcid.org/0000-0003-2397-5591
M. Błażewicz http://orcid.org/0000-0002-4753-3424
P. F. Clark http://orcid.org/0000-0001-6862-3982
F. Palero http://orcid.org/0000-0002-0343-8329

References

Baez P. 1973. Larvas phyllosoma del pacífico sur oriental (Crustacea, Macrura, Scyllaridea). Revista de Biologia Marina15(1):115–130.

Ballard JWO, Whitlock MC. 2004. The incomplete natural history of mitochondria. Molecular Ecology 13(4):729–744. DOI:10.1046/j.1365-294X.2003.02063.x.

Barber PH, Erdmann MV, Palumbi SR. 2006. Comparative phylogeography of three codistributed stomatopods: Origins and timing of regional lineage diversification in the coral triangle. Evolution 60(9):1825. DOI:10.1554/05-596.1.

Bouvier EL. 1909. Arctus Delfini sp. nov. Revista Chilena de Historia Natural. 13:213–215.

Boxshall GA. 2004. The evolution of arthropod limbs. Biological Reviews of the Cambridge Philosophical Society 79(2):253–300. DOI:10.1017/S1464793103006274.

Boxshall GA, Danielopol DL, Horne DJ, Smith RJ, Tabacaru I. 2010. A critique of biramous interpretations of the crustacean antennule. Crustaceana 83(2):153–167. DOI:10.1163/001121609X12530988607434.

Bracken-Grissom HD, Ahyong ST, Wilkinson RD, Feldmann RM, Schweitzer CE, Breinholt JW, Bendall M, Palero F, Chan TY, Felder DL, Robles R, Chu KH, Tsang LM, Kim D, Martin JW, Crandall KA. 2014. The emergence of lobsters: Phylogenetic relationships, morphological evolution and divergence time comparisons of an ancient group (Decapoda: Achelata. Astacidea, Glypheidea, Polychelida). Systematic Biology 63(4):457–479. DOI:10.1093/sysbio/syu008.

Buhay JE. 2009. 'Coi-like' sequences are becoming problematic in molecular systematic and DNA barcoding studies. Journal of Crustacean Biology 29(1):96–110. DOI:10.1651/08-3020.1.

Chan TY. 2012. A new genus of deep-sea solenocerid shrimp (Decapoda: Penaeoidea) from Papua New Guinea. Journal of Crustacean Biology 32(3):489–495. DOI:10.1163/193724012X626557.

Chan TY, Ahyong ST, Yang CH. 2013. Priority of the slipper lobster genus *Crenarctus* Holthuis 2002, over *Antipodarctus* Holthuis 2002 (Crustacea, Decapoda, Scyllaridae). Zootaxa 3701(4):471–472. DOI:10.11646/zootaxa.3701.4.7.

Cheng SH, Anderson FE, Bergman A, Mahardika GN, Muchlisin ZA, Dang BT, Calumpong HP, Mohamed KS, Sasikumar G, Venkatesan V, Barber PH. 2014. Molecular evidence for co-occurring cryptic linages within the *Sepioteuthis* cf. *lessoniana* species complex in the Indian and Indo-West Pacific Oceans. Hydrobiologia 725(1):165–188. DOI:10.1007/s10750-013-1778-0.

Clark PF, Calazans DK, Pohle GW. 1998. Accuracy and standardization of brachyuran larval descriptions. Invertebrate Reproduction and Development 33(2–3):127–144. DOI:10.1080/07924259.1998.9652627.

Coleman CO. 2003. 'Digital inking': How to make perfect line drawings on computers. Organisms Diversity and Evolution 3 (4):303–304. DOI:10.1078/1439-6092-00081.

Coleman CO. 2009. Drawing setae the digital way. Zoosystematics and Evolution 85(2):305–310. DOI:10.1002/zoos.200900008.

De Forges BR, Corbari L. 2012. A new species of *Oxypleurodon* Miers, 1886 (Crustacea, Brachyura, Majoidea) from the Bismarck Sea, Papua New Guinea. Zootaxa 3320:56–60.

De Man JG. 1905. Diagnososes of new species of Macrurous Decapod Crustacea from the 'Siboga-Expedition'. Tijdschrift der Nederlandsche Dierkundige Vereeniging 9(2):587–614.

DeBoer TS, Abdon Naguit MR, Erdmann MV, Ablan-Lagman MCA, Ambariyanto CKE, Toha AHA, Barber PH. 2014. Concordant phylogenetic patterns inferred from mitochondrial and microsatellite DNA in the giant clam *Tridacna crocea*. Bulletin of Marine Science 90(1):301–329. DOI:10.5343/bms.2013.1002.

Edgar RC. 2004. MUSCLE: Multiple sequence alignment with high accuracy and high throughput. Nucleic Acids Research 32(5):1792–1797. DOI:10.1093/nar/gkh340.

Folmer O, Black M, Hoeh W, Lutz R, Vrijenhoek R. 1994. DNA primers for amplification of mitochondrial cytochrom c oxidase subunit I from diverse metazoan invertebrates. Molecular Marine Biology and Biotechnology 3(5):294–299. DOI:10.1371/journal.pone.0013102.

Galtier N, Nabholz B, Glémin S, Hurst GDD. 2009. Mitochondrial DNA as a marker of molecular diversity: A reappraisal. Molecular Ecology 18(22):4541–4550. DOI:10.1111/j.1365-294X.2009.04380.x.

Garm A, Watling L. 2013. The crustacean integument: Setae, setules, and other ornamentation. In: Watling L, Thiel M, editors. Functional morphology and diversity. Oxford: Oxford University Press. pp. 167–198.

Genis-Armero R, González-Gordillo JI, Cuesta JA, Capaccioni-Azzati R, Palero F. 2020. Revision of the West African species of *Scyllarus* Fabricius, 1775 (Decapoda: Achelata: Scyllaridae), with the description of three phyllosoma stages of *S. caparti* Holthuis, 1952 and an updated identification key. Journal of Crustacean Biology 40(4):412–424. DOI:10.1093/jcbiol/ruaa025.

Gibson J, Shokralla S, Porter TM, King I, Van Konynenburg S, Janzen DH, Hallwachs W, Hajibabaei M 2014. Simultaneous assessment of the macrobiome and microbiome in a bulk sample of tropical arthropods through DNA metasystematics. Proceedings of the National Academy of Sciences 111 (22):8007–8012.

Guindon S, Dufayard JF, Lefort V, Anisimova M, Hordijk W, Gascuel O. 2010. New algorithms and methods to estimate maximum-likelihood phylogenies: Assessing the performance of Phy ML 3.0. Systematic Biology 59(3):307–321. DOI:10.1093/sysbio/syq010.

Hall T. 1999. Symposium on RNA Biology. III. RNA, Tool and Target. Research Triangle Park North Carolina, USA October 15-17, 1999 Proceedings

Hall R. 2002. Cenozoic geological and plate tectonic evolution of SE Asia and the SW Pacific: Computer-based reconstructions, model and animations. Journal of Asian Earth Sciences 20 (4):353–431. DOI:10.1016/S1367-9120(01)00069-4.

Haug JT, Audo D, Charbonnier S, Palero F, Petit G, Abi Saad P, Haug C. 2016. The evolution of a key character, or how to evolve a slipper lobster. Arthropod Structure and Development 45(2):97–107. DOI:10.1016/j.asd.2015.08.003.

Higa T, Shokita S. 2004. Late-stage phyllosoma larvae and metamorphosis of a scyllarid lobster, *Chelarctus cultrifer* (Crustacea:

Decapoda: Scyllaridae), from the Northwestern Pacific. Species Diversity 9:221–249.

Holthuis LB 1963. Preliminary descriptions of some new species of Palinuridea (Crustacea Decapoda, Macrura Reptantia). Proceedings Koninklijke Nederlandse Akademie van Wetenschappen, Series C 66:54–60. https://es.wikipedia.org/wiki/Proceedings_of_the_Koninklijke_Nederlandse_Akademie_van_Wetenschappen

Holthuis LB. 1985. A revision of the family Scyllaridae (Crustacea Decapoda Macrura). I. Subfamily Ibacinae. Zoologische Verhandelingen 218(218):1–130.

Holthuis LB. 1991. FAO species catalogue. Marine lobsters of the world. An annotated and illustrated catalogue of species of interest to fisheries known to date. FAO Fisheries Synopsis. No. 125. Vol. 13. Rome: FAO. p. 292 . https://www.fao.org/publications/card/en/c/5b06cf31-81fe-54f7-ac3c-5d4380638296/

Holthuis LB. 2002. The Indo-Pacific scyllarine lobsters (Crustacea, Decapoda, Scyllaridae). Zoosystema 24(3):499–683.

Hou Z, Li S. 2018. Tethyan changes shaped aquatic diversification. Biological Reviews 93(2):874–896. DOI:10.1111/brv.12376.

Inoue N, Sekiguchi H. 2006. Descriptions of phyllosoma larvae of *Scyllarus bicuspidatus* and *S. cultrifer* (Decapoda, Scyllaridae) collected in Japanese waters. Plankton and Benthos Research 1(1):26–41. DOI:10.3800/pbr.1.26.

Johnson MW. 1971. On Palinurid and Scyllarid lobster larvae and their distribution in the South China Sea (Decapoda, Palinuridea). Crustaceana 21(3):247–282. DOI:10.2307/20101842.

Johnson MW. 1979. On a north pacific *Scyllarus* phyllosoma larva with a forked telson (Decapoda, Scyllaridae). Bulletin of Marine Science 29(4):592–597.

Kochzius M, Nuryanto A. 2008. Strong genetic population structure in the boring giant clam, *Tridacna crocea*, across the Indo-Malay Archipelago: Implications related to evolutionary processes and connectivity. Molecular Ecology 17:3775–3787. DOI: 10.1111/j.1365-294X.2008.03803.x.

Krehenwinkel H, Kennedy SR, Rueda A, Lam A, Gillespie RG. 2018. Scaling up DNA barcoding – Primer sets for simple and cost efficient arthropod systematics by multiplex PCR and Illumina amplicon sequencing. Methods in Ecology and Evolution 9:2181–2193.

Kumar S, Stecher G, Li M, Knyaz C, Tamura K. 2018. MEGA X: Molecular evolutionary genetics analysis across computing platforms. Molecular Biology and Evolution 35(6):1547–1549. DOI:10.1093/molbev/msy096.

Latreille PA. 1825. Familles Naturelles du Règne Animal, expsées succinctement et dans un ordre analytique, avec l'indication de leurs genres. Paris.

Lohman DJ, de Bruyn M, Page T, von Rintelen K, Hall R, Ng PKL, Shih H-T, Carvalho GC, von Rintelen T. 2011. Biogeography of the Indo-Australian Archipelago. Annual Review of Ecology, Evolution, and Systematics 42:205–226. DOI: 10.1146/annurev-ecolsys-102710-145001.

Lourie SA, Green DM, Vincent ACJ. 2005. Dispersal, habitat differences, and comparative phylogeography of Southeast Asian seahorses (Syngnathidae: Hippocampus). Molecular Ecology 14 (4):1073–1094. DOI:10.1111/j.1365-294X.2005.02464.x.

Lourie SA, Vincent ACJ. 2004. A marine fish follows Wallace's line: The phylogeography of the three-spot seahorse (Hippocampus trimaculatus, Syngnathidae, Teleostei) in Southeast Asia. Journal of Biogeography 31(12):1975–1985. DOI:10.1111/j.1365-2699.2004.01153.x.

Maigret J. 1978. Contribution à l'étude des langoustes de la côte occidentale d'Afrique (Crustacés, Décapodes, Palinuridae). Bulletin de l'Institut Fondamental de l'Afrique Noire 40 (1):36–80.

Nguyen TTT, Murphy NP, Austin CM. 2002. Amplification of multiple copies of mitochondrial Cytochrome b gene fragments in the Australian freshwater crayfish, *Cherax destructor* Clark (Parastacidae: Decapoda). Animal Genetics 33(4):304–308. DOI:10.1046/j.1365-2052.2002.00867.x.

Ortmann AE. 1897. Carcinologische Studien. Zoologische Jahrbücher. Abteilung für Systematik, Geographie und Biologie der Thiere 10(3):258–372.

Palero F, Abello P. 2007. The first phyllosoma stage of *Palinurus mauritanicus* (Crustacea: Decapoda: Palinuridae). Zootaxa 1508(1508):49–59.

Palero F, Crandall KA, Abelló P, Macpherson E, Pascual M. 2009. Phylogenetic relationships between spiny, slipper and coral lobsters (Crustacea, Decapoda, Achelata). Molecular Phylogenetics and Evolution 50(1):152–162.

Palero F, Genis-Armero R, Hall M, Clark PF. 2016b. DNA barcoding the phyllosoma of *Scyllarides squammosus* (H. Milne Edwards, 1837) (Decapoda: Achelata: Scyllaridae). Zootaxa 4139(4):481.

Palero F, Guerao G, Abelló P. 2008. Morphology of the final stage phyllosoma larva of *Scyllarus pygmaeus* (Crustacea: Decapoda: Scyllaridae), identified by DNA analysis. Journal of Plankton Research 30(4):483–488.

Palero F, Guerao G, Hall M, Chan TY, Clark PF. 2014. The 'giant phyllosoma' are larval stages of *Parribacus antarcticus*. Decapoda : Scyllaridae. Invertebrate Systematics 28:258–276.

Palero F, Hall S, Clark PF, Johnston D, Mackenzie-Dodds J, Thatje S, Johnston J. 2010. DNA extraction from formalin-fixed tissue: New light from the Deep-Sea. Scientia Marina 74 (3):465–470.

Palero F, Robainas-Barcia A, Corbari L, Macpherson E. 2016a. Phylogeny and evolution of shallow-water squat lobsters (Decapoda, Galatheoidea) from the Indo-Pacific. Zoologica Scripta 46(5):584–595. DOI:10.1111/zsc.12230.

Palma ÁT, Cáceres-Montenegro I, Bennett RS, Magnolfi S, Henríquez LA, Guerra JF, Manríquez K, Palma RE. 2011. Near-shore distribution of phyllosomas of the two only lobster species (Decapoda: Achelata) present in Robinson Crusoe Island and endemic to the Juan Fernández archipelago. Revista Chilena de Historia Natural 84(3):379–390. DOI:10.4067/S0716-078X2011000300006.

Pante E, Corbari L, Thubaut J, Chan TY, Mana R, Boisselier MC, Bouchet P, Samadi S. 2012. Exploration of the deep-sea fauna of Papua New Guinea. Oceanography 25(3):214–225. DOI:10.5670/oceanog.2012.65.

Phillips BF, McWilliam PS. 1986. The pelagic phase of spiny lobster development. Canadian Journal of Fisheries and Aquatic Sciences 43:2153–2163.

Poore GCB, Andreakis N. 2011. Morphological, molecular and biogeographic evidence support two new species in the *Uroptychus naso* complex (Crustacea: Decapoda: Chirostylidae). Molecular Phylogenetics and Evolution 60 (1):152–169. DOI:10.1016/j.ympev.2011.03.032.

Schneider CA, Rasband WS, Eliceiri KW. 2012. NIH Image to ImageJ: 25 years of image analysis. Nature Methods 9 (7):671–675. DOI:10.1038/nmeth.2089.

Schubart CD. 2009. Mitochondrial DNA and decapod phylogenies: The importance of pseudogenes and primer optimization. In: Martin JW, Crandall KA, Felder DL, editors. Decapod crustacean phylogenetics. Boca Raton, London, New York: CRC Press. pp. 47–65.

Sekiguchi H. 1986. Spatial distribution and abundance of phyllosoma larvae in the Kumano- and Enshu-Nada seas north of

the Kuroshio Current. Bulletin of the Japanese Society of Fisheries Oceanography 50(4):289–297.

Sekiguchi H. 1990. Four species of phyllosoma larvae from the Mariana waters. Bulletin of the Japanese Society of Fisheries Oceanography 54(3):242–248.

Song H, Buhay JE, Whiting MF, Crandall KA. 2008. Many species in one: DNA barcoding overestimates the number of species when nuclear mitochondrial pseudogenes are coamplified. Proceedings of the National Academy of Sciences of the United States of America 105(36):13486–13491. DOI:10.1073/pnas.0803076105.

Tsoi KH, Chan TY, Chu KH. 2007. Molecular population structure of the kuruma shrimp *Penaeus japonicus* species complex in western Pacific. Marine Biology 150(6):1345–1364. DOI:10.1007/s00227-006-0426-x.

Tsoi KH, Chan TY, Chu KH. 2011. Phylogenetic and biogeographic analysis of the spear lobsters *Linuparus* (Decapoda: Palinuridae), with the description of a new species. Zoologischer Anzeiger 250 (4):302–315. DOI:10.1016/j.jcz.2011.04.007.

Ueda K, Yanagimoto T, Chow S, Kuroki M, Yamakawa T. 2021. Molecular identification of mid to final stage slipper lobster phyllosoma larvae of the genus *Chelarctus* (Crustacea: Decapoda: Scyllaridae) collected in the pacific with descriptions of their larval morphology. Zoological Studies 60(75):1–21.

Wakabayashi K, Yang C-H, Chan T-Y, Phillips BF. 2020. The final phyllosoma, nisto, and first juvenile stages of the slipper lobster *Petrarctus brevicornis* (Holthuis, 1946) (Decapoda: Achelata: Scyllaridae). Journal of Crustacean Biology March: 1–10. DOI:10.1093/jcbiol/ruaa013.

Webber WR, Booth JD. 2001. Larval stages, developmental ecology, and distribution of *Scyllarus* sp. Z (probably *Scyllarus aoteanus* Powell, 1949) (Decapoda: Scyllaridae). New Zealand Journal of Marine and Freshwater Research 35:1025–1056. DOI: 10.1080/00288330.2001.9517061.

Whitelegge T. 1900. Scientific results of the trawling Expedition of H.M.C.S. "Thetis" off the coast of New South Wales in February and March, 1898. Crustacea, Part 1. Australian Museum Memoir. 4(2):135–199.

Williams ST, Knowlton N. 2001. Mitochondrial pseudogenes are pervasive and often insidious in the snapping shrimp genus *Alpheus*. Molecular Biology and Evolution 18(8):1484–1493. DOI:10.1093/oxfordjournals.molbev.a003934.

Yang CH, Bracken-Grissom H, Kim D, Crandall KA, Chan TY. 2012. Phylogenetic relationships, character evolution, and taxonomic implications within the slipper lobsters (Crustacea: Decapoda: Scyllaridae). Molecular Phylogenetics and Evolution 62(1):237–250. DOI:10.1016/j.ympev.2011.09.019.

Yang CH, Chan TY. 2012. On the taxonomy of the slipper lobster Chelarctus cultrifer (Ortmann, 1897) (Crustacea: Decapoda: Scyllaridae), with description of a new species. Raffles Bulletin of Zoology 60(2):449–460.

Yu DW, Ji Y, Emerson BC, Wang X, Ye C, Yang C, Ding Z. 2012. Biodiversity soup: Metabarcoding of arthropods for rapid biodiversity assessment and biomonitoring. Methods in Ecology and Evolution 3(4):613–623.

Zaharias P, Kantor YI, Fedosov AE, Criscione F, Hallan A, Kano Y, Bardin J, Puillandre N. 2020. Just the once will not hurt: DNA suggests species lumping over two oceans in deep-sea snails (*Cryptogemma*). Zoological Journal of the Linnean Society 190(2):532–557. DOI:10.1093/zoolinnean/zlaa010.